Aalto University
School of Engineering

Methanol Production via CO_2 Hydrogenation

Eero Vesterinen

Supervisor: Prof. Martti Larmi

Advisor: M.Sc. Mohamed Magdeldin

Aalto University School of Engineering

Thesis submitted for examination for

the degree of Master of Science in Technology.

Espoo 26.11.2018

Aalto University
School of Engineering

Aalto University, P.O. BOX 11000, 00076
AALTO
www.aalto.fi

Abstract of master's thesis

Author Eero Vesterinen

Title of thesis Methanol Production via CO_2 Hydrogenation

Master programme Energy Technology **Code** ENG21

Thesis supervisor Professor Martti Larmi

Thesis advisor M.Sc. Mohamed Magdeldin

Date 26.11.2018 **Number of pages** 51 + 18 **Language** English

Abstract

Renewable and sustainable solutions in energy and transportation sector are under vast research and development to mitigate anthropogenic emissions and climate change. Alternative fuels to replace the conventional fossil fuel –based ones play an essential role to reduce the environmental impact in transportation. Methanol production based on renewable energy provides an interesting option in sustainable fuel production industry. In addition, methanol is extensively applied as a base component in chemical industry.

The first part of this thesis provides a literature review on pathways and equipment in methanol production. The second part focuses on a simulation of a methanol production process modelled in Aspen Plus software. A complete process configuration from CO_2 extraction from ambient air and hydrogen production by water electrolysis to methanol synthesis via CO_2 hydrogenation is included in the model. The results are analyzed focusing on viewpoints on material and energy consumption and process optimization.

The material and energy requirements in the considered scale (170 000 t of methanol per year) are substantially large especially if considering renewable energy sources exclusively. However, optimization of the processed streams could largely reduce the material consumption. A major share of the electricity consumption is induced by the hydrogen production step. Thus, (at least partial) hydrogen feedstock and/or electricity from other sources is suggested. Heat integration of the plant is investigated applying Aspen Energy Analyzer. The heating requirements of the entire process could be fulfilled with optimized heat integration and purge combustion in the synthesis/distillation step. However, the large amount of purges result in a relatively low carbon conversion rate (76,7 %). In general, the plant performance seems to be reasonable considering key values in efficiency (energy efficiency on LHV basis is 43,1 % and on HHV basis 50,0 %).

Keywords methanol, CO_2 hydrogenation, CO_2 capture from ambient air, water electrolysis, Aspen, simulation

Aalto-yliopisto
Insinööritieteiden
korkeakoulu

Aalto-yliopisto, PL 11000, 00076 AALTO
www.aalto.fi
Diplomityön tiivistelmä

Tekijä Eero Vesterinen

Työn nimi Metanolin tuotanto hiilidioksidin hydrauksella

Maisteriohjelma Energy Technology **Koodi** ENG21

Työn valvoja professori Martti Larmi

Työn ohjaaja diplomi-insinööri Mohamed Magdeldin

Päivämäärä 26.11.2018 **Sivumäärä** 51 + 18 **Kieli** englanti

Tiivistelmä

Uusiutuvat ja kestävät ratkaisut ovat energiantuotanto- ja liikennesektorilla laaja-alaisen tutkimus- ja kehitystyön kohteena ihmisperäisten päästöjen ja ilmastonmuutoksen hillitsemiseksi. Vaihtoehtoiset polttoaineet perinteisten fossiilisten polttoaineiden korvaamiseksi ovat olennaisessa asemassa liikenteen ympäristövaikutusten vähentämiseksi. Metanolin tuotanto uusiutuvan energian avulla on mielenkiintoinen ala kestävässä polttoaineteollisuudessa. Lisäksi metanolia hyödynnetään laajalti peruskemikaalina kemian tekniikassa.

Työn ensimmäinen osa sisältää kirjallisuuskatsauksen metanolin tuotannossa käytetyistä menetelmistä ja laitteistoista. Toinen osa keskittyy Aspen Plus –ohjelmistolla tehtyyn simulaatioon metanolin tuotannosta. Malli sisältää koko prosessiketjun hiilidioksidin talteenotosta ilmasta ja vedyntuotannosta vesielektrolyysin avulla synteesiin hiilidioksidin hydrauksella. Tulosten analysointi keskittyy näkökulmiin materiaalien ja energian kulutuksesta, sekä prosessioptimoinnista.

Prosessin materiaali- ja energiavaatimukset ovat huomattavia valitussa skaalassa (170 000 tonnia metanolia vuodessa) mikäli tarvittava energia olisi uusiutuvin keinoin tuotettua. Käytettyjen materiaalivirtojen optimointi kuitenkin pienentää suuressa määrin raaka-aineiden kulutusta. Selkeästi suurin osa sähköntarpeesta on peräisin vedyntuotantovaiheesta. Täten (ainakin osittainen) muualta saatu vety- ja/tai sähkövirta olisi suositeltua. Prosessin lämmönsiirtoverkon optimointia tutkittiin Aspen Energy Analyzer –työkalun avulla. Koko prosessin lämmöntarve pystytään täyttämään optimoidun lämmönsiirtoverkon ja synteesi-/tislausvaiheen ylijäämien polton avulla. Suuri ylijäämävirta kuitenkin johtaa suhteellisen alhaiseen prosessin hiilen konversioarvoon (76,7 %). Yleisesti ottaen prosessin tehokkuuden avainluvut ovat hyväksyttäviä (energiatehokkuus alemman lämpöarvon perusteella 43,1 % ja ylemmän lämpöarvon perusteella 50,0 %).

Avainsanat metanoli, hiilidioksidin hydraus, hiilidioksidin talteenotto ilmasta, vesielektrolyysi, Aspen, simulaatio

Foreword

This master's thesis was conducted as part of research in the Department of Energy Technology in Aalto University, Finland. I would like to thank professor Martti Larmi for his guidance and providing this interesting subject for the thesis, M.Sc. Mohamed Magdeldin for his sincere help and support and professor Annukka Santasalo-Aarnio for her comments and feedback. In addition, I would like to thank my friends, family and fellow students for being there and making this time spent in university a lot easier.

Espoo 26.11.2018

Eero Vesterinen

Table of contents

List of figures

List of tables

Abbreviations

CAMERE	Methanol synthesis process applying carbon dioxide hydrogenation via reverse water-gas shift reaction
DC	Direct current
DMFC	Direct methanol fuel cell
ENRTL-RK	Electrolyte non-random two-liquid Redlich-Kwong
HHV	Higher heating value
LHV	Lower heating value
MeOH	Methanol
MOF	Metal-organic frameworks
PEM	Polymer electrolyte membrane
PSRK	Predictive Soave-Redlich-Kwong
rWGS	Reverse water-gas shift
SOEC	Solid oxide electrolyser cell
STP	Standard temperature and pressure

Symbols

$\Delta H_{R,298K}$	Reaction heat in standard conditions
Nm^3	Newton cubic metre

1 Introduction

Climate change and diminishing fossil resources are globally increasing environmental awareness and interest in renewable and sustainable solutions. Low-emission technologies substituting the conventional fossil fuel-based methods are in an essential role in mitigating anthropogenic environmental impact. A major share of the greenhouse gas emissions originate from energy production and transportation. Thus, alternative fuels for replacing the traditional fossil fuels applied in transportation are under vast research and development. Among these, renewable methanol is one of the most promising options in sustainable fuel production industry.

The role of renewable methanol production may be different depending on the source of the renewable electricity and feedstocks applied in the process. Considering fluctuating electricity sources such as solar and wind power, large amounts of produced electricity are occasionally curtailed as a surplus electricity when the demand is low. Thus, methanol production may be applied as an energy storage method to compensate the differences between demand and supply. However, dynamic operation of a methanol production plant may not be feasible and electricity storage or additional electricity from the grid would probably be required. Considering steady-state renewable energy sources such as geothermal energy, methanol production is a valid application for fuel production exploiting conventional process equipment.

Methanol (CH_3OH) is the simplest form of alcohols. In STP conditions, it is a clear liquid-state chemical (boiling point at 64,7 ^oC and melting point at -97,7 ^oC). As a liquid-state chemical, methanol may be feasibly stored and transported with the existing infrastructure. The primary applications for methanol cover three different categories: exploitation as a fuel, raw material feedstock for synthetic hydrocarbons and electricity production in a direct methanol fuel cell (DMFC). In fuel applications, methanol may be blended with gasoline. However, both the volumetric and specific energy densities of methanol are approximately half of those for gasoline and diesel. (Olah, 2005)

This thesis consists of two major parts. First, a literature review about different methanol production methods and equipment is provided. The second part of the thesis provides an investigation about a simulation modelled with Aspen Plus software. The model includes an entire methanol production process via carbon dioxide hydrogenation. The investigated process covers the whole production scheme from CO_2 extraction and hydrogen production finally resulting in distilled high purity methanol. The results are analysing the feasibility of the process together with energy efficiency and mass balance calculations.

2 Pathways in methanol production

This chapter introduces several methanol production processes. In addition, carbon dioxide extraction and hydrogen production processes are examined as methanol production via CO_2 hydrogenation is the focus in this study.

The primary processes applied in methanol production are hydrogenation from syngas, reductive conversion of CO_2 with hydrogen and direct oxidative conversion of methane. For the last few decades, practically every commercial application for methanol production has been operated applying a two-stage process where natural gas (essentially methane) was first converted to syngas and then to methanol. (Gesser et al. 1985) The syngas has traditionally been obtained by coal gasification but steam methane reforming of natural gas is currently the most applied method in syngas production. However, any material containing coal may be applied as a feedstock for methanol production. (Frilund 2016) (Olah 2005)

In renewable methanol production, similar pathways may be followed. The primary processes for renewable methanol production are introduced in Figure 2.1. In general, carbon and hydrogen feedstocks are required in any methanol production process. Renewable carbon feedstocks provide options for production of syngas and/or pure CO_2. Hydrogen may be produced in several methods such as natural gas reforming and water splitting methods such as electrolysis. (DOE) Considering sustainable hydrogen production, electricity from renewable sources is typically applied in water electrolysis resulting in pure hydrogen and oxygen streams. (Galindo Cifre, Badr 2007)

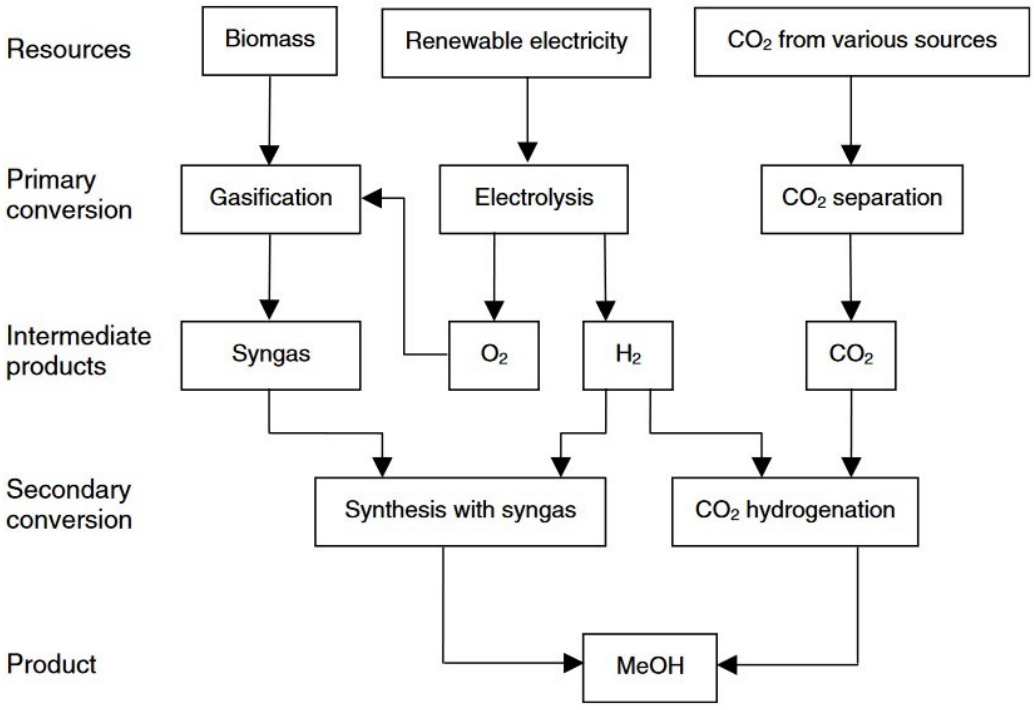

Figure 2.1. Primary pathways in renewable methanol production. (Galindo Cifre, Badr 2007)

2.1 Carbon dioxide hydrogenation

In carbon dioxide hydrogenation, methanol is produced applying pure CO_2 and H_2 streams as feedstock. Methanol production from pure CO_2 feedstock follows three primary reactions. In addition to the CO_2 hydrogenation reaction, the reverse water gas-shift reaction is present resulting in carbon monoxide and water. The produced carbon monoxide is further hydrogenated into methanol via another hydrogenation reaction. The reaction rates are dependent on the applied catalyst and operational conditions. (Frilund 2016)

The three primary reactions occurring in carbon dioxide hydrogenation to methanol are:

CO_2 hydrogenation:

$$CO_2 + 3\,H_2 \leftrightarrows CH_3OH + H_2O \qquad \Delta H_{R,298K} = -49{,}5 \text{ kJ/mol} \qquad \text{(Eq. 2.1)}$$

Reverse water-gas shift:

$$CO_2 + H_2 \leftrightarrows CO + H_2O \qquad \Delta H_{R,298K} = 41{,}0 \text{ kJ/mol} \qquad \text{(Eq 2.2)}$$

CO hydrogenation:

$$CO + 2\,H_2 \leftrightarrows CH_3OH \qquad \Delta H_{R,298K} = -90{,}5 \text{ kJ/mol} \qquad \text{(Eq 2.3)}$$

(Frilund 2016)

Additionally, an approach to methanol production from CO_2 is the CAMERE process where methanol is produced via CO_2-to-CO process. However, this process is proven to be less energy- and economically efficient than the direct hydrogenation of CO_2. As seen in the CO_2 hydrogenation reaction, one third of the hydrogen is converted into water, thus resulting in a large non-desirable by-product yield. (Frilund 2016)

2.1.1 Carbon dioxide extraction

Stationary applications such as (especially fossil fuel -based) energy production and cement industry are among the largest contributors for anthropogenic CO_2 emissions, in addition to mobile sources such as transportation. (EPA) Consequently, CO_2 capture applications are principally located along major point sources such as fossil fuel -fired power plants and cement production facilities. Pre-, oxy- and post-combustion capture processes are the three most mature methods for CO_2 capture considering power plants. (Leung et al. 2014) In cement industry, post-combustion and oxy-combustion processes are the most promising applications as pre-combustion techniques are too impractical to be applied in the phase (limestone conversion to calcium oxide) in which most of the CO_2 is emitted. (Meunier et al. 2014)

Various other methods have been developed to produce a pure CO_2 stream, as well. Considering this research, CO_2 capture from ambient air provides interesting possibilities as such applications may be situated in any location. Consequently, direct air capture equipment may be connected with the primarily discussed power sources, solar and wind power, which are often dependent on the location.

2.1.1.1 Carbon dioxide capture from ambient air

CO_2 capture from ambient air provides several desirable possibilities in producing a CO_2 feedstock and reducing the CO_2 content in the atmosphere. The method is unrestricted considering location as CO_2 emissions are rapidly mixed with air and diluted and conveyed around the globe. As a "last resort" capture method ignoring the source of emissions, direct air capture is mitigating the fundamental problem of increase in the greenhouse gas concentrations in the atmosphere and even reducing the effect of past emissions. Additionally, atmospheric carbon dioxide may be considered as an abundant feedstock. (Lackner 2009)

The price estimations in literature for direct air capture of CO_2 largely differ from each other and the method is often discussed not to be economically feasible. However, various sources provide an estimation that is competitive with the average price for CO_2 extracted with conventional methods. (Sanz-Pérez et al. 2016) The process applied as the fundamental scheme for this research provided by Keith et al. (2018) is estimated to result in a cost of 94-232 USD/t of CO_2 depending on the configuration and possible operational connections in the complete plant design.

2.1.1.2 Sorbents

Several sorbent types have been proven to be appropriate for CO_2 capture in various, fossil-fuel based flue gas, applications. However, the CO_2 concentration in atmosphere is naturally much lower than in the flue gases from fossil fuel combustion. A large share of the sorbents designed for flue gas cleaning offer a poor performance when the CO_2 concentration is reduced. Among the applied sorbents in CO_2 extraction, chemisorbents such as calcium hydroxide, sodium hydroxide and potassium hydroxide provide the best efficiency when processing a feedstock of low CO_2 concentration. (Sanz-Pérez et al. 2016)

Most of the current direct air capture applications are applying sodium hydroxide as a sorbent. Such configurations are employing or variating the Kraft process that has been exploited, originally by paper industry, since the late 19th century. Applications utilizing potassium hydroxide as a sorbent follow similar methods to the NaOH processes. In a technical viewpoint, the only major difference is to apply KOH and K_2CO_3 instead of NaOH and Na_2CO_3 in the carbon capture loop. The carbonate compound is then reacting with calcium hydroxide ($Ca(OH)_2$) to form calcium carbonate ($CaCO_3$) which is heated to release the captured CO_2. The remaining calcium oxide (CaO) is then reacting with steam to obtain the required calcium hydroxide. (Sanz-Pérez et al. 2016) Potassium-based configurations provide a decrease in the sorbent regeneration temperature compared to processes applying sodium hydroxide as a sorbent. (Goeppert et al. 2012)

Aqueous amine solutions are among the most traditional sorbents applied in gas phase CO_2 separation from sources with high CO_2 concentration. For direct air capture of CO_2, solid-supported amine sorbents are currently the most studied materia. The chemical reaction between CO_2 and the amines creates strong bonds and allows high uptake rates when processing gas streams of low CO_2 concentration. Consequently, these organic-inorganic hybrid sorbents provide high selectivity and heat of sorption towards CO_2, thus being favourable for direct CO_2 capture from ambient air. (Sanz-Pérez et al. 2016)

Poly(ethylenimine) has been the sorbent under primary research focus. It is an amine-containing polymer providing a large density of amine groups and desirable stability under temperature swing

adsorption and vacuum swing adsorption conditions, Typically, poly(ethylenimine) is applied as oxide compounds to achieve higher stability considering sorbent recycling and thermal conditions. Several studied silica-based sorbents with different (33 %-50 %) poly(ethylenimine) loads provided the best CO_2 uptake values at temperatures similar to atmospheric conditions (max. 50 ^oC). The CO_2 capture potential of these sorbents drastically decreased with increased temperatures. (Sanz-Pérez et al. 2016)

In addition to temperature, the moisture of the processed air has an impact on the efficiency of poly(ethylenimine) sorbents. Typically, the CO_2 adsorption potential of amines increases in the presence of water by allowing bicarbonates to formate. However, the effect of moisture variates depending on the poly(ethylenimine) concentration in the sorbent. In a study performed by Goeppert et al. (2011), a sorbent of 33 % poly(ethylenimine) concentration increased its CO_2 adsorption rate when increasing the moisture in the processed air. On the contrary, the CO_2 adsorption rate of a sorbent of 50 % poly(ethylenimine) concentration decreased with higher moisture content in the processed air. (Goeppert et al. 2011)

Metal-organic frameworks (MOFs) have been applied in CO_2 adsorption, as well. Shekhah et al. (2014) proposed a novel recyclable MOF composition that provides high adsorption capacity and selectivity towards CO_2 in both low and high CO_2 concentrations, thus being suitable for air capture applications. Additionally, this MOF sorbent indicated no decrease in performance when studied with increased humidity levels.

2.2 Hydrogen production

The methods in conventional hydrogen production are primarily based on fuel processing technologies. The typical processing methods apply reforming or gasification technologies, reforming of hydrocarbons (mainly steam reforming of methane) being the most exploited process. Considering low emission hydrogen production, water electrolysis coupled with renewable electricity is typically applied. (Holladay et al. 2009)

In water electrolysis, the water molecules are split with the aid of an electrical current following the simple overall reaction:

$$H_2O \leftrightarrows H_2 + 1/2\ O_2 \qquad \Delta H_{R,298K} = -288\ kJ/mol \qquad \text{(Eq. 2.4)}$$

(Holladay et al. 2009)

The most applied process for water electrolysis is alkaline electrolysis that has been in commercially available for several decades. Additionally, polymer electrolyte membrane (PEM) electrolysers are applied in commercial installations. Along with PEM electrolysis, anion exchange membrane electrolysis is under research and development. For steam electrolysis, solid oxide electrolysis cells (SOEC) are under research, as well. (Mergel et al. 2013)

2.2.1 Alkaline electrolysis

In alkaline electrolysis, water is typically fed to the electrolyser on the cathode side where it splits into hydrogen and hydroxide ions. The hydroxide ions are transported through a liquid alkaline electrolyte (typically an aqueous KOH solution) to the anode side where they react into oxygen, water and electrons. (Mergel et al. 2013) The operational principles of alkaline electrolysis are introduced in Figure 2.2.

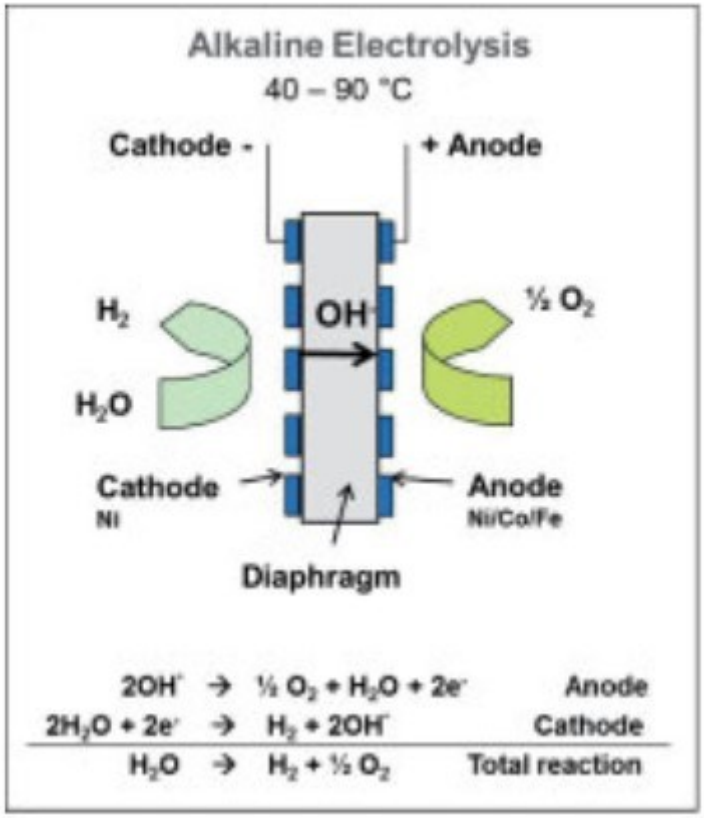

Figure 2.2. The operational principles of alkaline electrolysis. (Mergel et al. 2013)

Typical energy requirements and current densities in alkaline electrolysis range between 4-5 kWh/Nm^3 of H_2 and 0,2-0,4 A/m^2. The operational temperature ranges between 40-90 °C. Higher efficiencies and more reliable operation may be achieved in higher temperatures. (Mergel et al. 2013)

Alkaline electrolysers have proven to successfully operate at intermittent loads. The electrolyser power may be relatively effortlessly adjusted by adapting the current density. However, side-electrolysis phenomenon determines a certain minimum load for every alkaline electrolyser. Depending on the electrolyser type, the minimum load is usually estimated to be 20-25 % under which the side-electrolysis may not be neglected. Additionally, alkaline electrolysers do not react instantaneously to load changes and discontinuous operation may conduct some additional degradation of the equipment. (Mansilla et al. 2011)

2.2.2 Polymer electrolyte membrane electrolysis

In polymer electrolyte membrane (PEM) electrolysis, water is split into oxygen, protons and electrons by applying a DC voltage that is higher than the thermoneutral voltage of the electrolyser. Typically, water is fed to a PEM electrolyser on the anode side. (Mergel et al. 2013) The oxygen is collected from the anode side and the protons pass through the electrolyte membrane to combine with electrons to form hydrogen on the cathode side. Thus, the PEM electrolysis process is similar, but reverse, to the process occurring in a PEM fuel cell. (Barbir 2005)

PEM electrolysers are argued to reach higher performance in a dynamic operational context than the more conventional alkaline electrolysers. The solid polymer membrane responds more rapidly to fluctuating input power than the liquid alkaline electrolyte and the normal operational load range of PEM electrolysers is larger than that of alkaline electrolysers. Additionally, the system design is more compact due to the lack of liquid electrolyte and additional equipment required in an alkaline electrolyser system. (Koponen 2015) However, costful components (noble metal catalysts and expensive components such as membranes, current collectors and separator plates) required in the process together with its lower state of development induce high expenses for PEM electrolysers compared to alkaline electrolysers. (Mergel et al. 2013)

2.2.3 Solid oxide electrolyser cells

Solid oxide electrolyser cells (SOECs) provide a more desirable performance compared to PEM and alkaline electrolysis as it produces a higher chemical reaction rate for hydrogen demanding less electrical energy. SOEC electrolysers operate at higher temperatures than equipment for water electrolysis due to the ceramic components which are conductive only at high temperature levels. Thus, thermal energy is required in addition to the electricity and the processed water is in the form of steam. The high temperature level, especially in the product gases, provides opportunities to utilize the waste heat from the process. A potential option for waste heat recovery is to preheat the feed water by a heat exchanger. (Ni et al. 2008)

The primary components of a SOEC consist of two porous electrodes and a dense ionic conducting electrolyte between them. The processed steam is fed to the cathode. Under a required electrical potential, the steam diffuses to the reaction sites and dissociates to hydrogen gas and oxygen ions at the cathode-electrolyte interface. The obtained hydrogen is collected at the cathode surface and the oxygen ions are conducted through the electrolyte to the anode where they are oxidized to oxygen gas. (Ni et al. 2008)

2.3 Conversion from methane

Methane is currently the primary carbon feedstock in methanol production. Several pathways for methanol production from methane may be followed. Two-stage conversion from methane is presently the most common method. In addition, direct conversion methods are applied.

2.3.1 Two-stage conversion

At present, the most applied method to produce methanol exploiting a feedstock of natural gas (essentially methane) is via a two-stage conversion process. The first step of the process is to convert the natural gas into syngas. Secondly, methanol is produced from the syngas via

hydrogenation. The operating temperatures and pressures required for exploiting this process are substantially high. Thus, large amount of energy is required to complete the process. Adding large capital costs for the equipment, the method is economically feasible only for large-scale applications.

2.3.1.1 Methane-syngas

Various different processes are applied in methane conversion to syngas. The two most common processes in industrial applications are steam methane reforming and (catalytic) partial oxidation. Depending on the process configuration, multiple conversion technologies may be combined to improve the application performance. (Baltrusaitis, Luyben 2015)

2.3.1.1.1 Steam methane reforming

Steam methane reforming is a widely applied syngas generation process with an extensive industrial experience. The process is capable to produce syngas with a high hydrogen content (H_2:CO ratio of ~3) which is an advantage considering methanol production industry where similar ratios are required. Steam methane reforming process is largely endothermic and favours high temperature and low pressure conditions. (Baltrusaitis, Luyben 2015) However, the process temperature in steam methane reforming is low compared to other available technologies for syngas generation. (Wilhelm et al. 2001)

The primary reaction in steam methane reforming is:

$$CH_4 + H_2O \leftrightarrows CO + 3\,H_2 \qquad \text{(Eq. 2.5)}$$

Steam-to-methane (H_2O:CH_4) molar ratios of 3 are typical for steam methane reforming applications. Increasing steam-to-methane feed ratio or/and temperature conduct higher methane conversion rates. (Baltrusaitis, Luyben 2015)

The large amount of high temperature steam has high energy requirements and induces corrosion in reactor equipment. Adding the expensive process infrastructure, the syngas process is costful and typically responsible for 60 to 70 % of total methanol production costs. (da Silva 2016)

2.3.1.1.2 Dry methane reforming

Dry methane reforming process provides an end product stream including carbon monoxide and hydrogen in a one-to-one ratio. In the process, methane reacts with carbon dioxide following a primary reaction of:

$$CH_4 + CO_2 \leftrightarrows 2\,CO + 2\,H_2 \qquad \text{(Eq. 2.6)}$$

Dry methane reforming process is largely endothermic requiring much additional heating. Similarly to steam methane reforming, methane conversion rate is favoured by increased temperature and low pressure. (Baltrusaitis, Luyben 2015)

2.3.1.1.3 Autothermal reforming

In autothermal reforming, an oxygen stream is fed to the reactor inducing a partial oxidation reaction for methane. The heat from this exothermic reaction of is further exploited in to supply the required heat in the endothermic reforming reaction. The autothermal reforming process supports reduction of CO_2 emissions due to the lack of external heating equipment. The partial oxidation process conducts a need for larger methane feed and a relatively expensive oxygen feedstock. However, the capital cost for an autothermal reforming unit is typically less expensive than for steam reforming. (Baltrusaitis, Luyben 2015)

2.3.1.1.4 Partial oxidation of methane to syngas

The primary feedstocks for partial methane oxidation processes consist of methane and oxygen. Compared to steam reforming , partial oxidation process produces a syngas stream of lower H_2/CO ratio (typically from 1 to 1,6). Catalytic partial oxidation processes typically operate at lower temperatures (below 800 ^oC) than non-catalytic ones which are operated at temperatures above 1 200 ^oC. (Baltrusaitis, Luyben 2015)

The primary reaction in partial oxidation of methane to syngas is:

$$CH_4 + 1/2\ O_2 \leftrightarrows CO + 2\ H_2 \qquad \Delta H_{R,298K} = -36\ kJ/mol \qquad \text{(Eq. 2.7)}$$

(York et al. 2003)

The typical catalysts for partial oxidation process are supported nickel, cobalt, iron or noble metal, and transition metal carbide compounds. For oxidative methane-syngas conversion, two general methods have been studied over metal catalysts:

- Combustion and reforming reactions mechanism, which is an indirect conversion mechanism in which methane is first totally combusted and steam and dry reforming reactions are added downstream in the process

- Direct partial oxidation mechanism, which is a direct oxidation mechanism in which surface carbon and oxygen compounds form the primary products

(York et al. 2003)

2.3.1.2 Methanol hydrogenation from syngas

Syngas refers to a mixture of hydrogen, carbon monoxide and carbon dioxide. When applied as a feedstock for methanol production, the composition of the syngas has an explicit impact on the reaction kinetics and resulting yields from the process. Methanol hydrogenation from syngas follows the same primary reactions as methanol production via CO_2 hydrogenation (Eq. 2.1-2.3).

The process is rather sensitive to various parameters such as thermodynamic conditions and the CO_2 concentration of the syngas. Thus, specific catalysts and recycling of the unreacted gases are typically required to reach desirable methanol yields. Low-temperature catalysts are among the primary research subjects in the field. (Frilund 2016)

- High CO_2 concentration: Water-gas shift reaction progresses only in reverse direction, reducing the amount of CO_2 and increasing the water concentration. Low methanol yields and extremely poor methanol selectivity.

- Moderate CO_2 concentration: Forward water-gas shift reaction active. High CO_2 hydrogenation rate. Selectivity to methanol slightly decreased and water production net rate slightly increased.

- Low CO_2 concentration: Limited methanol formation. Water-gas shift reaction active in forward direction.

- Very low CO_2 concentration: Catalytic activity significantly reduced. Increased potential for catalyst deactivation, carbon deposition and/or catalyst oxide reduction.

(Lee, Sardesai 2005)

Co-production of methanol and dimethyl ether may significantly increase the reactor productivity. Dual catalysts designed for this co-production process perform high activities and reduced deactivation potential. (Lee, Sardesai 2005)

2.3.2 Direct oxidation

The two-stage conversion of methane to methanol is still the dominant process in methane-methanol applications but direct oxidation of methane provides several advantages over the two-stage process. Direct oxidation of methane to methanol is more energy-efficient compared to two-stage conversion via syngas, and results in a liquid methanol yield in only one step. The main reaction in this process is the following:

$$CH_4\,(g) + 1/2\,O_2\,(g) \leftrightarrows CH_3OH\,(l) \qquad \Delta H_{R,298K} = -30{,}7 \text{ kcal} \qquad \text{(Eq. 2.8)}$$

(Gesser et al. 1985)

The reaction may be executed in both gas and liquid phases. (Zakaria, Kamarudin 2016)

The direct methane-to-methanol oxidation process has been under vast research over the last century. However, the conversion rate and selectivity for methanol have remained as a challenge. (Han et al. 2016) The main approaches in the research for direct methane oxidation are conversion process techniques in low temperature and pressure conditions, and different catalyst applications.

2.3.2.1 Heterogeneous oxidation

In heterogeneous methane-methanol oxidation, a catalyst (typically a transition metal oxide compound) is added to support the conversion process. The most widely studied catalysts are based on molybdenum trioxide and iron compounds. (Han et al. 2016)

2.3.2.2 Homogeneous gas phase oxidation

In addition to catalytic processes, direct oxidation of methane to methanol may be achieved non-catalytically via homogeneous oxidation in gas phase. The reaction is fundamentally dependant on the process temperature and pressure. The process initial temperature has to be high enough (above 400 ºC) to initiate the oxidation chain reaction, but the equilibrium temperature should be below a certain limit (550 ºC) to avoid further oxidation of the oxygenates. High pressure (typically 10-80 bar) is necessary for decent process conditions. An increase in the process pressure conducts an increase in methanol yield due to the process kinetics and typically reduces the optimal temperature for methanol selectivity. (Han et al. 2016)

2.3.2.3 Aqueous homogeneous oxidation

Aqueous homogeneous oxidation is a method applicable for converting methane to methanol resulting in a relatively high end product yield in mild conditions. However, a significant drawback in the process is that a major share of the currently discovered mediums necessary for the applications are strong acids (such as trifluoroacetic acid) and thus corrosive and seriously contaminant. Eliciting a sustainable medium is one of the main research subjects in the process examination. A few environmentally friendly solvents have been proposed and experimentally proven to reach suitable catalytic properties and high selectivity for methanol, but they are still examined only in experimental scale and far from exploitation in industrial applications.
(Han et al. 2016)

2.4 Other methanol production methods

In addition to the typical methanol production methods, several novel pathways for methanol production are studied. Among these, CO_2 capture from air with direct conversion to methanol and bio-catalysis are introduced here.

2.4.1 Carbon dioxide capture from air and direct conversion to methanol

Kothandaraman et al. (2015) studied direct CO_2 conversion to methanol over a novel catalyst after capture from ambient air. Instead of poly(ethylenimine), they applied pentaethylenehexamine (PEHA) as an ethereal sorbent. A ruthenium-based catalyst was introduced to convert the reaction mixture to methanol after CO_2 capture. The presence of polyamines occasionally deactivate the catalyst in similar processes. However, no significant catalyst deactivation was observed in this process configuration. On the contrary, both the catalyst and PEHA sorbent provided excellent recycling properties. The catalyst performed at 75% of the initial activity after 5 cycles in the hydrogenation process.

The examined application seemed to provide efficient results in CO_2 hydrogenation from synthetic air, providing methanol at a 79% conversion rate. Applying a triglyme/H_2O mixture, process temperature of 155 ºC and pressure of 50 bar resulted in a 61 % methanol yield. The 79 % methanol yield was achieved after additional heating. (Kothandaraman et al. 2015)

2.4.2 Bio-catalysis

Direct conversion of methane to methanol may be achieved with the aid of enzyme-catalysed reactions, as well. These natural catalysts are named as methane mono-oxygenase enzymes. The advantages of these enzymes include their high product selectivity and ability to operate in ambient conditions. However, the drawbacks include low activity for methanol production and the requirement for an expensive reductant supply. (Kondratenko et al. 2017) (Zakaria, Kamarudin 2016)

Methane mono-oxygenase enzymes may be divided into two subgroups, soluble methane mono-oxygenase enzymes and particulate methane mono-oxygenase enzymes. Soluble methane mono-oxygenase enzymes require a nicotinamide adenine dinucleotide reductant as an electron donor in the process but particulate methane mono-oxygenase enzymes may exploit electrons from ubiquinol (coenzyme Q10), as well. (Kondratenko et al. 2017)

3 Equipment for methanol synthesis and distillation

This chapter introduces some of the typical and more novel equipment applied in methanol synthesis and distillation.

3.1 Synthesis reactors

Various different reactor types may be applied for methanol production processes. Currently, packed bed reactors are the most employed reactor type for methanol synthesis and may be applied for methanol production from various feedstocks. (Frilund 2016) Fluidized bed membrane reactors are among the more novel reactor types under research. (van der Ham et al. 2012)

Typical operating temperatures and pressures in methanol synthesis range between 200-300 ºC and 50-100 bar. The reaction is regulated by the limits of chemical equilibrium resulting in an incomplete conversion. Thus, the synthesis process configuration typically contains a recycle system for the unreacted components. As the reactor outlet stream is in gaseous phase, the reacted mixture is cooled down before the separation of the recycle stream. The separation is typically performed in a gas-liquid flash separator as the recycled components (primarily CO_x and H_2) are still in a gaseous form and the liquid form product stream (primarily methanol and water) is sent to distillation. (Kiss et al. 2016) A simplified typical synthesis process configuration is introduced in Figure 3.1.

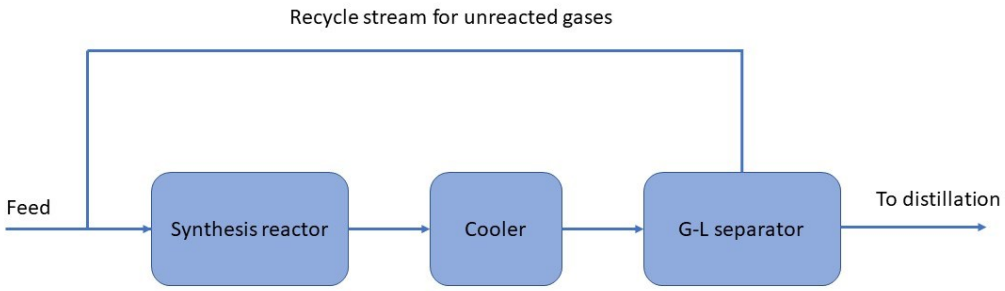

Figure 3.1. Simplified typical process configuration for methanol synthesis.

3.1.1 Packed bed reactors

Packed bed reactors, or fixed bed reactors, are tubular reactors containing a bed of solid catalyst. They are designed for heterogeneous catalytic reactions and are applied for gas-solid, liquid-solid and gas-liquid-solid reactions. Packed bed reactors may be applied in either adiabatic or isothermal operation. Isothermal packed bed reactors are typically multitubular to allow higher heat transfer performance and cooled with water. (Frilund 2016)

As the synthesis reaction is highly exothermic, effective and continuous heat transfer is required to maintain the desired temperature level. The reactor design largely resembles that of a heat exchanger. (Tijm et al. 2001) A typical packed bed reactor design is introduced in Figure 3.2.

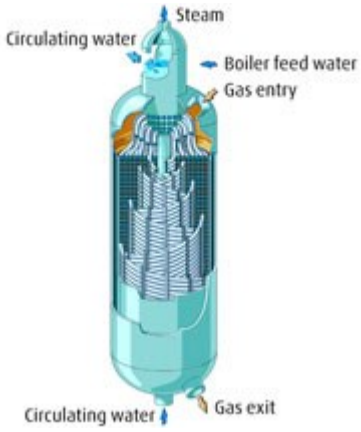

Figure 3.2. Typical packed bed reactor design. (The Linde Group 2018)

The most employed catalyst for methanol synthesis in packed bed reactors seems to be a $Cu/ZnO/Al_2O_3$ -compound. Studt et al. (2014) examined the behaviour of Ni-Ga -based catalysts in a packed bed reactor. The investigated catalysts seem to overcome the conventional $Cu/ZnO/Al_2O_3$ -catalysts considering several aspects, especially when operated in temperatures above 220 °C. The primary advantage is that Ni-Ga -catalysts increase the methanol yield by reducing the reverse water-gas shift reaction rate compared to Cu-Zn -catalysts which induce high rates of rWGS. Among the examined Ni-Ga -catalysts, Ni_5Ga_3/SiO_2 is particularly active towards methanol synthesis.

Wang et al. (2011) examined various catalysts for CO_2 hydrogenation covering a large number of different metal-based catalysts, focusing on variations of Cu-Zn -catalysts. In their research, Cu/pentane/NC-ZnO -compound operated at 450 °C reached the highest CO_2 conversion rate (80 %). Additionally, they discovered multiple substances that may be combined with the traditional $Cu/ZnO/Al_2O_3$ -catalyst to improve its performance.

3.1.2 Two-stage catalyst bed reactor

Two-stage reactor concepts allow optimizing equipment size by decreasing the recycle ratio and improving heat integration between the two reactor stages. They are typically applied in large-scale systems where these properties are important in process optimization. Lurgi MegaMethanol technology provided by Air Liquide Engineering & Construction is among the most applied

reactor types in commercial plants. The two-stage Lurgi MegaMethanol process is introduced in Figure 3.3.

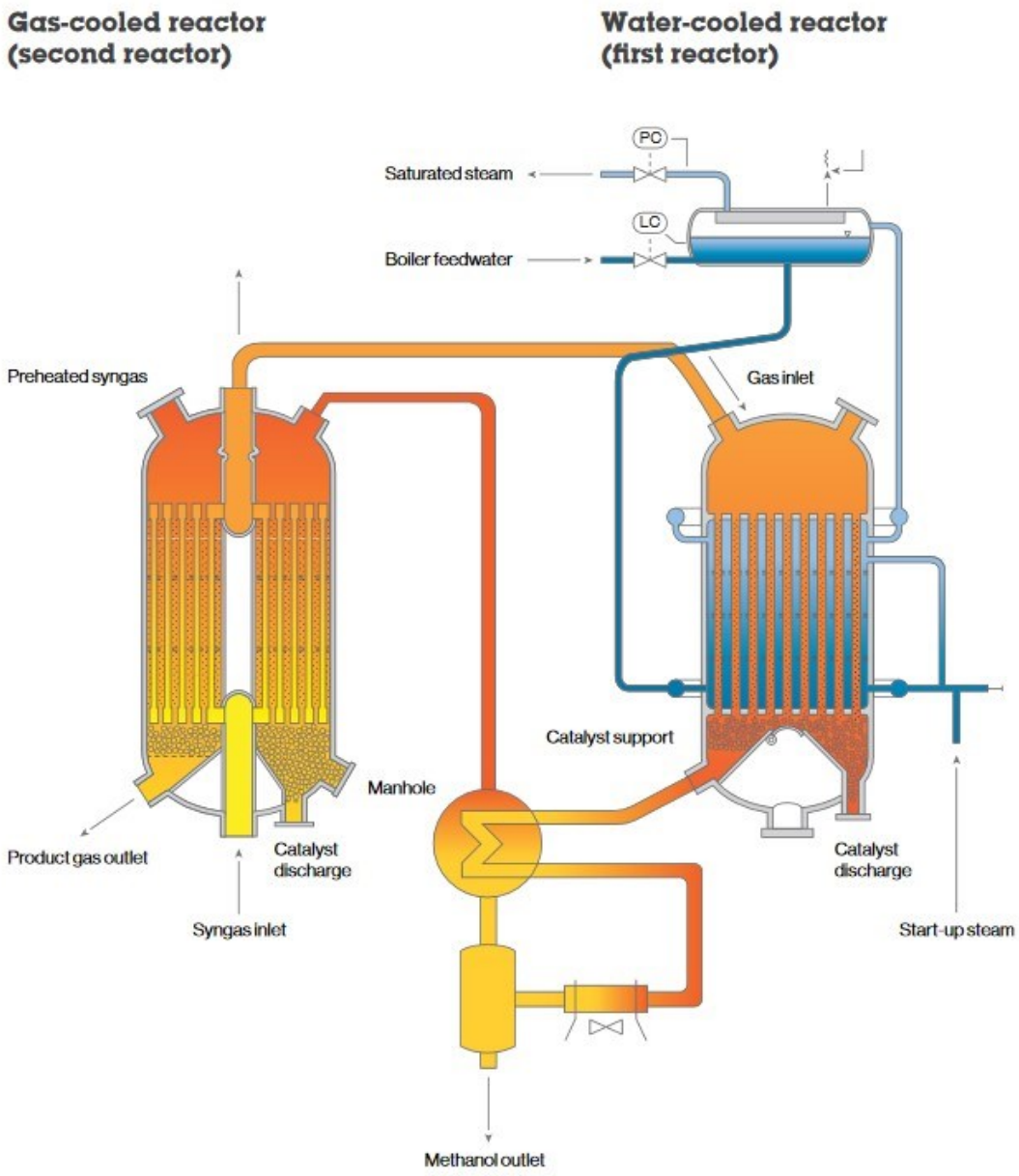

Figure 3.3. Lurgi MegaMethanol two-stage process design.

Rahimpour (2008) examined a two-stage catalyst bed reactor concept corresponding the Lurgi MegaMethanol process. The model seems to overcome the traditional single-bed reactor considering certain attributes. The most desirable advantages compared to the single-bed reactor include more favourable temperature profile, higher conversion rate and longer catalyst lifetime.

The first stage of the two-stage model is similar to a conventional water-cooled one-stage reactor, but operated in a higher temperature and high yield. In the second bed, the operating temperature

continuously reduces to provide an increasing thermodynamic equilibrium potential. The reaction rate is much lower in the second bed inducing less reaction heat that is applied to pre-heat the feed gas to the first bed. Milder temperature profiles in the second bed provide less extreme conditions for the catalysts, thus preventing the catalyst deactivation via sintering. (Rahimpour 2008)

3.1.3 Fluidized bed membrane reactor

Van der Ham et al. (2012) researched the operation of a fluidized bed membrane reactor in the scale of 10 kt/y methanol production. Additionally, Rahimpour and Alizadehhesari (2008) examined similar processes in their study about two-stage fluidized bed membrane reactor concept, combining some advantages of both two-stage and fluidized bed membrane technologies. In their process configuration, the fluidized bed membrane technology is applied in the second, gas-cooled, reactor while the first reactor remains as a conventional, water-cooled, packed bed reactor. This model seems to result in more preferable heat and mass transfer properties in the reactor. Deactivation of the catalyst is generally a primary issue considering the reactor design, as well. In a fluidized bed membrane reactor, the deactivated catalyst may effortlessly be removed and regenerated. (van der Ham et al. 2012)

In their design, van der Ham et al. applied the mentioned $Cu/ZnO/Al_2O_3$ -compound in the membrane to operate as a catalyst. The process temperature is optimized to 250 °C. Higher process temperatures would destruct the membranes and lower process temperatures would result in low conversion levels. To control the process temperature, the reactor is applied with a water-cooling system through the reactor walls. (van der Ham et al. 2012)

The designed process produces a desirable conversion rate for methanol. Van der Ham et al. report that the membrane type selection and the energy needed for hydrogen compression and CO_2 separation as critical process items.

3.1.4 Coated catalytic reactors

Coated catalytic reactors are among the most researched subjects in the field of CO_2 hydrogenation to methanol at the moment. These reactors provide potential in improving small-scale renewable methanol synthesis applications. The main difference compared to the conventional reactor types is to apply the catalyst as a porous layer on the walls or other surface structure in the reaction chamber. (Frilund 2016)

3.2 Distillation

After methanol synthesis, the resulted crude methanol stream typically contains large amounts of water, some ethanol, dimethyl ether, and other impurities. Thus, distillation is required to reach methanol of high purity level. Methanol concentrations above 99 % may be obtained by applying appropriate distillation equipment.

The crude methanol stream contains both low-boiling and high-boiling (boiling points above and below the boiling point of methanol) undesired components. Thus, at least two distillation columns operating at different temperatures are required to remove the impurities. Various distillation processes have been developed depending on the plant configuration but many of them follow a similar path. Typically, the reactor outlet stream is first cooled down to a temperature in which

methanol is in liquid form. The low-temperature outlet stream is then inserted in a flash block to separate the gaseous components (CO, CO_2 and H_2) which are further recycled back to the reactor inlet stream. The resulting liquid stream consisting mostly of methanol and water is then processed in distillation and stripper columns to remove the water and other impurities.

The typical amount of the columns applied has increased from the past. (Ott et al. 2012) Currently, a standard methanol distillation application consists of three or four columns. Adding more columns to the distillation arrangement increases the capital cost of the equipment. However, the energy savings conduct notable reduction in the operating costs, allowing the more complicated applications to be economically even more feasible. (Sun et al 2012)

Distillation requires much energy as the process includes heat and mass transfer of considerable extent. Thus, energy-efficient solutions are desired and possible, typically applying heat recovery between the distillation columns. The energy-efficiency potential seems to increase when adding the number of columns. Novel five-column distillation schemes have been reported to achieve significant energy savings compared to four-column applications. (Sun et al. 2012) (Zhang et al. 2010)

Sadeghi and Ahangar (2012) studied a three-column distillation unit in a dynamic operation. Temperature and pressure are the main variables that affect the volatility of the components in the distilled composition. Thus, a reasonable amount of control over the operational variable, especially temperature and pressure, is required to achieve the highest efficiency in the distillation. This is emphasized in dynamic operation. Controlling the variables enhances the system performance, consequently facilitating energy savings and thermal load reductions, as well as decreasing the costs.

4 Modelling Approach

This chapter introduces the model for simulating a methanol production plant via carbon dioxide hydrogenation. In the model, the whole process from CO_2 extraction and hydrogen production via CO_2 hydrogenation resulting in distilled high purity methanol is covered. With the considered methods, the model is resulting in a novel configuration considering the complete process design.

The simulation is conducted applying commercial Aspen Plus V8.8 software. (AspenTech) It provides extensive tools to model chemical processes and their thermodynamic features. The software includes comprehensive background data considering various components and thermodynamic model sets applicable for different types of processes. The examined process is modelled in the software as a flowsheet consisting of suitable block (such as reactors or separators) and stream (such as material or heat) icons. When the required input data is inserted, the software simulates the process considering the given specifications and provides process data such as flow rates and energy requirements. The process behaviour may be examined by various analytical tools such as sensitivity analyses and optimizing variators, as well. The model includes a few Design-Spec blocks which are an example of an analytical tool, iterating a fitting value for the selected input to match the determined specifications for a dependent variable elsewhere in the model.

4.1 Description

The simulation is investigating the feasibility of methanol production exploiting electricity from renewable (primarily solar and wind) power sources. The examined process may be divided into three major process blocks in the flowsheet: carbon dioxide extraction, hydrogen production and methanol synthesis together with distillation. The renewable electricity is mainly consumed in the hydrogen production step requiring large amounts of energy.

The simulation is performed applying PSRK (predictive Soave-Redlich-Kwong) property method set except the hydrogen production phase where ENRTL-RK (electrolyte non-random two-liquid Redlich-Kwong) is applied due to the presence of electrolyte modelling. PSRK property method allows to model processes where a mixture of non-polar (such as CO_2) and polar (such as water) compounds are operated in high temperatures and pressures in adequate accuracy. ENRTL-RK property method provides a comprehensive background for modelling processes including electrolytes and solvents of either high or low concentration.

The model is scaled to produce 170 000 t of 99,6 % purity methanol per year. This corresponds to the initial capacity of Porvoo biodiesel refinery plant operated by Neste Oil when it commenced its operation in 2007. (Hydrocarbons Technology) The capacity equals to 21 250 kg/hr production rate when assuming a typical amount of 8 000 annual operational hours.

4.2 Carbon dioxide extraction

The carbon dioxide extraction is performed by direct air capture, based on a novel configuration provided by Keith et al. (2018). This method is selected as it enables reducing the CO_2 content in the atmosphere. Thus, no external CO_2 source (conventionally fossil fuel –based applications) are not required. Additionally, direct air capture is not restricted considering location and the configuration is applying the same medium (KOH) as the capturing sorbent that is applied as the

electrolyte in the hydrogen production process introduced in chapter 4.3. The configuration is reported to result in a notable decrease in economical costs compared to the previous cost estimations on direct air capture applications.

The process consists of two connected chemical loops applying potassium hydroxide as the capturing sorbent. In the potassium loop, the aqueous potassium hydroxide (KOH) sorbent captures the CO_2 from the ambient air blown through the air contactor (block "CONTACTO" in the flowsheet) resulting in potassium carbonate (K_2CO_3) and water. The solution is conveyed to the pellet reactor (block "PELLETRE") where the potassium carbonate reacts with calcium hydroxide ($Ca(OH)_2$) forming calcium carbonate ($CaCO_3$) and potassium hydroxide recycled back to the air contactor. The calcium carbonate washer applied after the pellet reactor is modelled as a separator block to simulate the actual performance of the equipment, separating the remaining potassium hydroxide with the water and releasing the gaseous impurities. To release the gaseous CO_2, the calciner (block "CALCINER") has to operate at high temperature (in this case, 900 ^oC). The calcium carbonate stream is first dried and heated to 300 ^oC applying the heat from the steam slaker. Before the calciner, the stream is still pre-heated in two steps exploiting the heat from the hot CO_2 stream. Further heating in the calciner dissociates the compound into calcium oxide and gaseous CO_2. The required heat is provided by combustion of methane introduced to the calciner. The resulting calcium oxide (CaO) is transported into the steam slaker (block "SLAKER") where it reacts with added steam to form calcium hydroxide required in the pellet reactor. The simplified process configuration is introduced in Figure 4.1 and the Aspen flowsheet for the CO_2 extraction process is introduced in Figure 4.2.

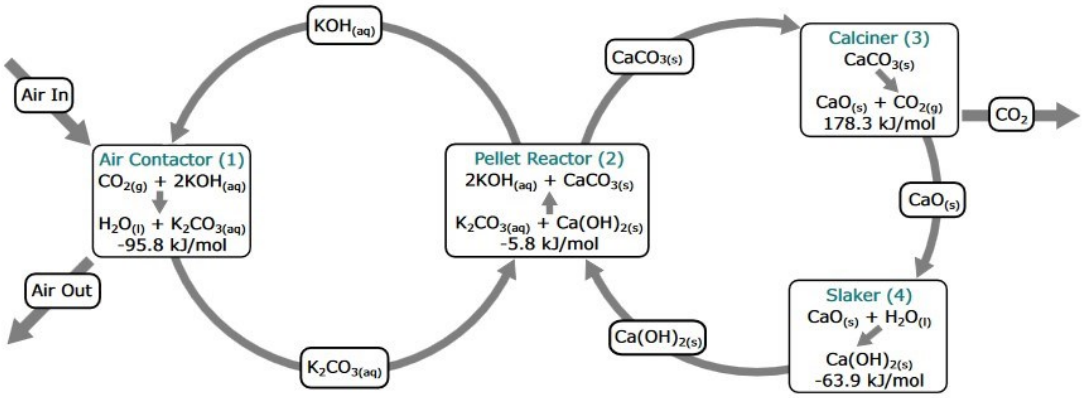

Figure 4.1. A simplified illustration of the CO_2 capture process. (Keith et al. 2018)

The gas turbine system in the design reported by Keith et al. (2018) providing power to the system and a flue gas stream for the CO_2 capture equipment is not included to decrease the dependence on fossil fuels and more compact process design. This results in a decrease in the produced CO_2. However, the decrease is relatively low compared to the amount of CO_2 obtained from the ambient air. Additionally, the $CaCO_3$ loop cycled through the filters and connected to the pellet reactor is ignored for simplification as it does not affect the $CaCO_3$ mass balance in the system.

The four main units (air contactor, pellet reactor, calciner and steam slaker) are each modelled as an adiabatic RStoic reactor block. A separator block (Flash2 or Separator) is added after each of

these units to model the separation of the different product streams. Additionally, the quicklime mix tank is modelled as an RStoic block as the remaining calcium oxide is mixed in it with water to provide the amount of calcium hydroxide required in the pellet reactor. The properties of the main units are introduced in Table 4.1.

Table 4.1. The main units in the CO_2 capture process.

Unit	**Name**	**Aspen block type**	**T, [°C]**	**p, [bar]**	**Main reaction, conversion efficiency** (Keith et al. 2018)
Air contactor	CONTACTO	RStoic	20	1	$2\ KOH + CO_2 \rightarrow K_2CO_3 + H_2O$, 74,5% conversion of CO_2
Pellet reactor	PELLETRE	RStoic	20	1	$K_2CO_3 + Ca(OH)_2 \rightarrow 2\ KOH + CaCO_3$, 90% conv. of $Ca(OH)_2$
Calciner	CALCINER	RStoic	900	1	$CaCO_3 \rightarrow CaO + CO_2$, 98% conv. of $CaCO_3$
Steam slaker	SLAKER	RStoic	300	1	$CaO + H_2O \rightarrow Ca(OH)_2$, 85% conv. of CaO

The streams “LIME-IN” and “LIME-OUT” are representing the aqueous $Ca(OH)_2$ stream introduced to the pellet reactor. The streams are separate to simulate the $Ca(OH)_2$ input to the process, thus being connected in actual system. Similarly, streams “SORB-IN” and “SORB-OUT” are representing the sorbent cycle for the air contactor and pellet reactor and connected in actual design. They are left unconnected to maintain a degree of freedom for the model to solve.

Compared to the original design by Keith et al. (2018), the heat exchanger network is simplified in the model so that only one heat exchanger per stream is applied. This is done to allow Aspen Energy Analyzer to find the best configuration for heat integration in this design. The energy analysis is introduced in chapter 5.4.

The resulting CO_2 stream is fed to a 4-stage compressor applied with inter-stage coolers and scrubbers removing most of the moisture in the stream to achieve the desired high purity CO_2. The compressor outlet pressure is set to 50 bar to match the reactor pressure in the synthesis phase.

The model includes three Design-Spec blocks for determining input values for certain streams to match the operational conditions reported by Keith et al. (2018). Block “CH4FLW” determines the mass flow rate for the combusted methane to achieve 900 °C operational temperature in the calciner. Block “O2FLW” determines the mass flow rate for oxygen so that the mass fraction of oxygen in the stream leaving the calciner (“S9”) equals to the reported value. Block “STEAMFLW” determines the mass flow rate for steam fed to the slaker to achieve 300 °C operational temperature.

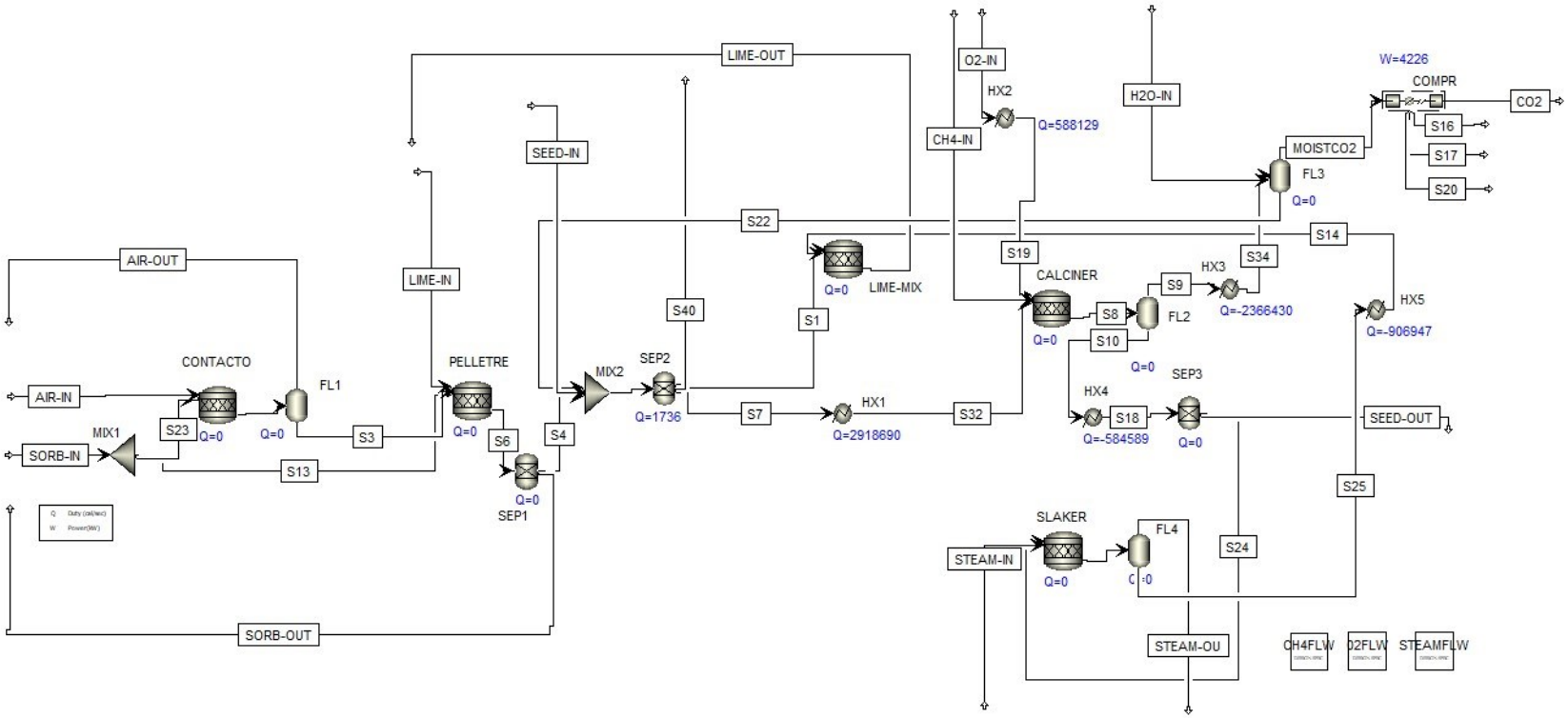

Figure 4.2. Aspen flowsheet of the CO_2 capture process.

4.3 Hydrogen production

The hydrogen production is performed by alkaline water electrolysis that is a well-known process and extensively applied in industrial applications. Electricity as direct current is applied to split water to the high purity hydrogen required in the methanol synthesis and oxygen released as a side product. Similarly to the CO_2 extraction model, potassium hydroxide acts as the alkaline in the solution provided to the electrolyser. The electrolyser is modelled based on reported information of equipment (Nel C-300 electrolyser) by Nel Hydrogen (2017). The electrolyser configuration is introduced in Figure 4.3.

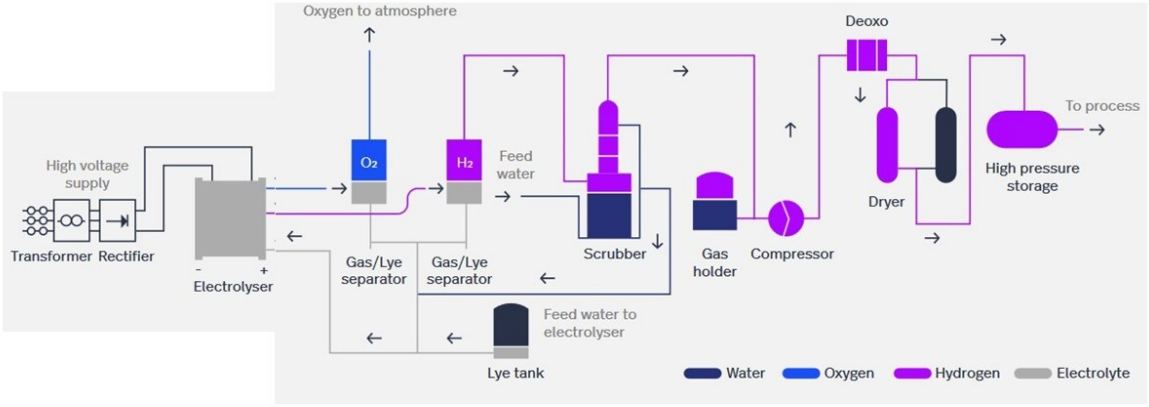

Figure 4.3. The electrolyser process configuration. (Nel Hydrogen 2017)

The aqueous electrolyte mix of 25% KOH concentration is fed to the electrolyser (block "ELECTR") that is modelled as an RStoic reactor block. The product stream leaving the electrolyser enters the "H2RCV" Flash2 block separating the wet hydrogen stream from the liquid form residual stream consisting mostly of the unreacted aqueous electrolyte and oxygen. The residual stream is then separated in "O2RCV" separator block to the electrolyte mix that is recycled to the process and high purity oxygen stream. The wet hydrogen is forwarded to "GASSCRUB" RadFrac block removing major share of the moisture in the gas. The dry hydrogen is then compressed in the "COMPRESS" multi-stage compressor block to 30 bar pressure. The compressed hydrogen is fed to the deoxidiser unit ("DEOX") modelled as an RStoic block where the remaining oxygen traces combine with hydrogen resulting in some moisture in the "DEOXGAS" product stream. The stream is fed to "DRYER" separator block removing the moisture and providing a high purity hydrogen stream containing only traces of impurities (moisture and oxygen).

The flowsheet contains two Design-Spec blocks. Block “SCRBFLW” determines the mass flow rate for the scrubbing water (stream “SCRBWT”) so that the temperature in the scrubbed hydrogen stream (stream “GAS”) is cooled down to 26 ^{o}C before compression. Block “DRYFRAC” defines the split fraction for moisture in the separator block “DRYER” so that the moisture resulting in the high purity hydrogen stream “PUREHYDR” equals to the reported value by Nel Hydrogen (2017).

The Aspen flowsheet of the hydrogen production process is introduced in Figure 4.4.

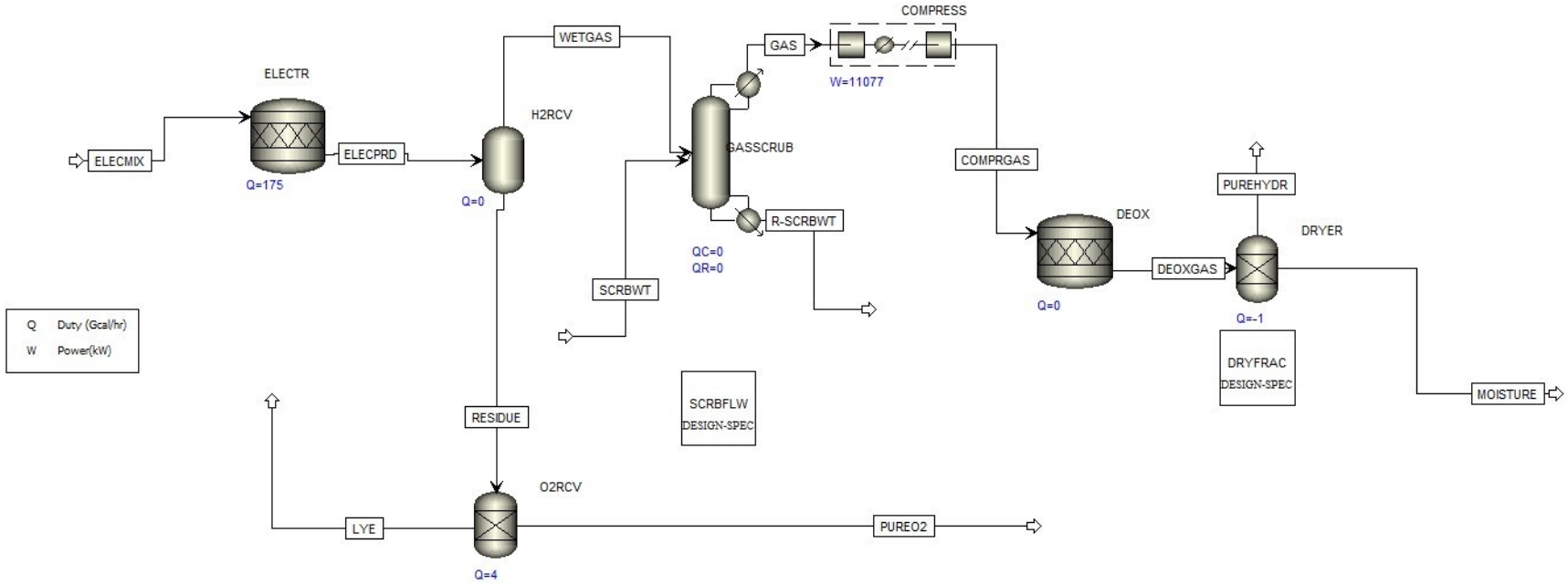

Figure 4.4. Aspen flowsheet for the water electrolysis in hydrogen production.

4.4 Methanol synthesis and distillation

The synthesis process is modelled as a typical methanol synthesis configuration including a recycle loop for the gases remaining unreacted after the reactor. The reactor feed consists of three streams (hydrogen, carbon dioxide and recycle streams) mixed before entering the reactor. The hydrogen stream leaves the hydrogen production process at 30 bar pressure which is increased before mixing in a compressor to 50 bar that is equivalent to the reactor conditions. After mixing, the feed stream is heated to 225 ºC before it is fed to the reactor. The methanol synthesis reactor is modelled as an RStoic reactor block (block "REACTOR") representing a typical isothermal fixed bed reactor cooled by an external water stream. After the reactor, the product stream temperature is decreased to 40 ºC to achieve liquid form for the components (primarily methanol and water) sent to distillation. The unreacted gaseous components are separated from these in a gas-liquid flash separator operated in 45 bar pressure to maintain system pressure and reduce compression demand and recycled back to the reactor feed stream after purge and compressor. The Aspen flowsheet of the distillation process together with the methanol synthesis process is introduced in Figure 4.5.

Three of the primary reactions occurring in methanol synthesis via carbon dioxide hydrogenation are considered in the reactor model. These reactions are CO_2 hydrogenation, CO hydrogenation and reverse water-gas shift. Typical side-reactions such as dimethyl ether and ethanol formation are ignored for simplicity and their minor presence in common methanol synthesis reactors.

The reaction rates required as an input in the RStoic reactor model are achieved by a sensitivity analysis and comparison with a process configuration provided by Kiss et al. (2016) similar to the examined scheme considering the general design. The operating temperature and pressure are determined to be 250 ºC and 50 bar which are similar to the reaction conditions in the configuration by Kiss et al. (2016) and represent typical values found in literature for similar applications. The reaction rates are dependent on the applied catalyst. In the study by Kiss et al. (2016), a fibrous Cu/Zn/Al/Zr catalyst was applied. Thus, the same catalyst is considered in this research.

Following reaction rates are applied as input for the reactor block: CO_2 hydrogenation: 0.099, reverse water-gas shift: 0.087 and CO hydrogenation: 1. Thus, CO_2 conversion rate (per pass) is defined as 17,6 % which resembles the values reported in the study by Kiss et al. (2016) (17,2 %) and elsewhere in literature. The difference may be explained and is affected by catalyst and equipment selection and other process optimization. All the carbon monoxide produced in the reverse water-gas shift reaction is hydrogenated in the following reaction as there should be no CO make-up in the process.

The reaction rates are determined based on a sensitivity analysis comparing the reactor inlet and outlet stream compositions with those of a largely similar scheme reported by Kiss et al. (2016). An error analysis focusing on the differences in CO_2 and H_2 conversion rates, methanol yield and reactor heat generation per feed mass flow ignoring the non-reactants N_2 and O_2 is applied as a basis for the selection. A 25 % weight factor is given to each of these error components. The chosen reaction rate values are the ones inducing the smallest error and providing a CO_2 conversion rate per pass resembling (<1% difference) the reported value in the compared scheme by Kiss et al. (2016). The error analysis results are presented in Appendix 1.

The composition of the reactor inlet stream differs to some extent compared to the composition in the background model reported by Kiss et al. (2016). This is primarily due to the presence of nitrogen and oxygen resulting from the methane combustion in CO_2 extraction. In actual process, the oxygen in the feed might result in issues such as oxidation reactions in the reactor. This should be considered but is excluded from this study. Hydrogen and carbon dioxide are inserted in the reactor in a 2,99:1 molar ratio (H_2:CO_2) which is similar to the stoichiometric equilibrium value and values proven to result in efficient conversion rates in literature. (Frilund 2016) (Kiss et al. 2016)

The purge in the recycle stream is set to 5 % which is relatively large value for typical synthesis configuration. This is due to the stream convergence calculation performed in Aspen that induces warning/error messages when reducing the purge value. The value could be decreased by a different stream convergence method. In this design, the purges from the recycle loop and first distillation column are combined and combusted in an RStoic reactor block (block "BOILER") to benefit from these large flow rates that would otherwise be considered as losses.

The distillation phase is modelled as a typical three-column application. Crude methanol stream is achieved after the first knockout drum (block "FL1") separating and recycling the unreacted gases. The liquid form crude methanol then enters another knockout drum (block "DIST1") operated in ambient pressure releasing more of the dissolved and unreacted gases as purge. The second distillation column is modelled with a RadFrac block (block "DIST2") and separates most of the water in the crude methanol stream. The next RadFrac block (block "DIST3") is operated as a steam stripper removing a major share of the remaining water and resulting in a high purity methanol stream. The distillation equipment is operated in atmospheric pressure but the steam applied in the last column is inserted in elevated pressure.

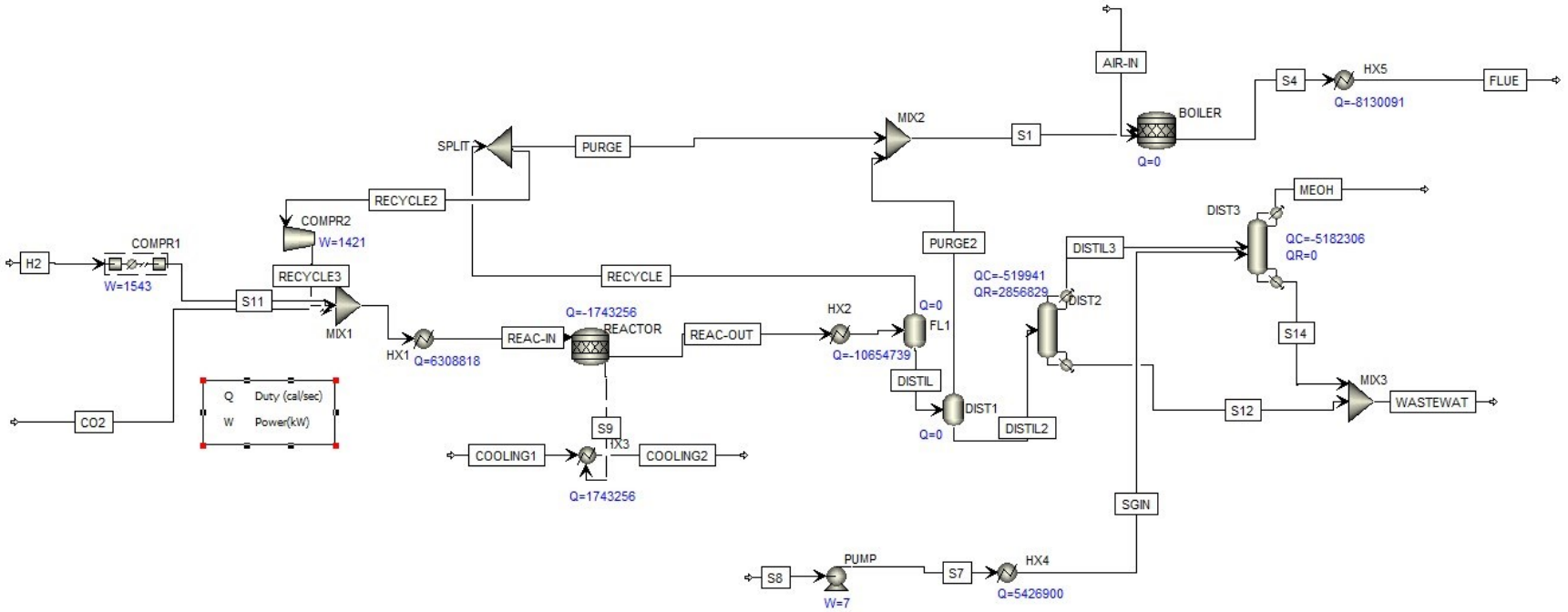

Figure 4.5. Aspen flowsheet of the synthesis and distillation processes.

4.5 Validation

An essential key figure for every process phase is examined and compared to values from studies applied as background/comparison to validate that the simulation model is realistic. These values are introduced in Table 4.2. The values are largely similar to each other but some differences are found primarily due to different process configurations. Proportionally, the largest difference is found in the CO_2 extraction process. This may be explained by excluding the external combustion of methane for power generation that is proposed in the original design and provides an increase in obtained CO_2 from its flue gases.

Table 4.2. Key figures for model validation.

Process phase	**Parameter**	**Simulated value**	**Comparison value**
CO_2 extraction	Produced CO_2 / processed air	0,000615 kg/kg	0,000681 kg/kg (Keith et al. 2018)
H_2 production	Feed water consumption	0,939 l / Nm^3 H_2	0,9 l / Nm^3 H_2 (NEL Hydrogen, 2017)
Methanol synthesis	Reactor heat generation / feed (ignoring O_2 & N_2)	128,4 kJ/kg	131,3 kJ/kg (Kiss et al. 2016)
Distillation	Methanol purity	0,996	1,00 (Kiss et al. 2016)

The main units in CO_2 capture, hydrogen production and methanol synthesis are modelled as RStoic reactor blocks. These reactor models consider reaction extent and stoichiometry but reaction kinetics are not inserted. This is assumed to be sufficient for this research as the extent and stoichiometry of the main reactions are achieved from literature and a sensitivity/error analysis introduced in chapter 4.4.

The simulation model includes Separator blocks that force the separation of different components in the material stream. Thus, they are not directly representing any actual equipment but may model actual processes in a more simplified manner. In this case, the inserted Separator blocks are applied for simplification to model the reported separations and not impacting the configuration in non-realistic means. The included separator blocks and their operational backgrounds are listed in Table 4.3.

Table 4.3**.** List of the separator blocks in the model.

Block name	**Process block**	**Modelling purpose**
SEP1	CO_2 capture	Separating the sorbent recycle stream
SEP2	CO_2 capture	Imitating the $CaCO_3$ pellet washer separating the solids and aqueous stream containing potassium compound remains and releasing the gases
SEP3	CO_2 capture	Separating the $CaCO_3$ seed stream fed to the pellet reactor
O2RCV	H_2 production	Representing the gas/lye separator producing high purity O_2 and electrolyte mix recycle streams
DRYER	H_2 production	Representing the dryer removing most of the moisture from the H_2 product stream

5 Results

This chapter provides the results from the simulation of the considered methanol production process. In addition to the key figures for each process block, the examination of results focuses on calculations about energy and material consumption and viewpoints on process optimization.

5.1 Carbon dioxide extraction

The capacity of the examined CO_2 extraction process is roughly a quarter of the capacity in configuration reported by Keith et al. (2018) considering both the amount of produced CO_2 and processed air. In their report, Keith et al. estimate a minimum capacity of 100 kt/a of CO_2 produced to achieve economical feasibility. The configuration in this research requires a production capacity more than 300 kt/a of CO_2, thus exceeding the reported value for economically feasible minimum capacity. However, the decrease in capacity is reported to result in higher costs per amount of produced CO_2, primarily considering capital cost of the calciner equipment. Key input and output figures for the CO_2 capture process are introduced in Table 5.1 and the extracted stream data from Aspen is introduced in Appendix 2.

A methane stream is combusted in the calciner to fulfill the heat requirement for the CO_2 release and provide an increase in the produced CO_2. Similar configuration is introduced in the original report by Keith et al. (2018). Applying renewable-based CH_4 should be considered to reduce the dependence on fossil fuels. The amount of required methane is achieved by a Design-Spec block so that the operational temperature in the calciner matches the defined value (900 ºC). The value is relatively large, resulting in an issue considering the infrastructure for supplying the required methane.

Table 5.1. Key input and output figures for the CO_2 capture process.

Parameter	**Value**	**Unit**
Produced CO_2 (from air and CH_4 in total)	39 721,4	kg/hr
CO_2 captured from air	29 526,4	kg/hr
Processed air	64 649,1	t/hr
Required CH_4	3 034,6	kg/hr
Required O_2	12 856	kg/hr
Required water	162,0	t/hr

An electricity consumption value of 8,84 MW is determined by dividing the reported values with the scale factor added with the value for compressor obtained from Aspen. The configuration in this research differs to some extent from the reported design as some of the equipment from the original design are excluded. Thus, only the electricity consumption from the applied equipment is considered.

The amount of required water is large. It consists of the water inserted to the knockout drum (block "B13") together with the water makeup in the steam slaker.

In addition to the reported $CaCO_3$ makeup in the filter system connected to the pellet reactor, the $CaCO_3$ seed circulated in the process should not require any additional makeup considering the original design from Keith et al. (2018). In the simulation, stream "SEED-OUT" is not providing a mass flow rate equal to the stream "SEED-IN" even though all the $CaCO_3$ remaining from the calciner is separated to it. Thus, an additional makeup of 149,3 kg $CaCO_3$/hr should be considered (in addition to the reported makeup).

In the original design, the quicklime is circulating in the process and would not require any makeup besides material degradation. However, the model results for streams "LIME-IN" and "LIME-OUT" differ from each other to some extent. The primary differences may be found in the flow rates of water and potassium-based solutions. Thus, some makeup would be required based on the Aspen results.

The produced CO_2 stream contains some oxygen and nitrogen resulting from the methane combustion in the calciner. Most of the moisture in the stream is removed in the knock-out drum and compressor. However, some moisture still remains in the product stream. The composition of the produced CO_2 stream is introduced in Table 5.2.

Table 5.2. Composition of the produced CO_2 stream.

Component	**Mass fraction**
CO_2	0,964
O_2	0,0189
N_2	0,0149
H_2O	0,0020

5.2 Hydrogen production

The required amount of hydrogen to reach the considered methanol production capacity equals to 5 066,5 kg/hr or 57 115 Nm^3/hr. This corresponds to 190,4 times the production capacity (300 Nm^3/hr) of the Nel C-300 electrolyser applied as a background for the model. (Nel Hydrogen 2017) The requirement for the added water flow equals to the amount of split water in the electrolyser as only oxygen is released as a side product and the potassium hydroxide is recycled. The required amount of water flow added in the system may be attained by the difference between the electrolyser inlet stream and the recycle stream and equals to 53 640 kg/hr. Key input and output figures for the hydrogen production process are introduced in Table 5.3.

The electricity consumption of hydrogen production in an electrolyser is substantially large as the process is essentially based on electrical current. The reported DC power consumption of the electrolyser is 3,8-4,4 kWh/Nm^3. (Nel Hydrogen 2017) Thus, the power requirement for the

considered hydrogen production process lies in the range between 217-251 MW. The applied pressure for hydrogen leaving the electrolyser is lower of the reported two values (30 bar/200 bar). The report by Nel Hydrogen (2017) does not explicitly define the sources for the power demand (e.g. if compressor power demand is included). The power consumption value is assumed to equal to 217 MW which is similar to the power consumption of the electrolyser and the compressor provided by the Aspen simulation (203,77 MW + 11,1 MW = 214,87 MW). The plant scale is substantially large considering that it is in a similar scale to the size of the purposed capacity of the Notodden facility in Norway currently under expansion that would provide a 360 MW annual production capacity, thus being the globally largest electrolyser plant. (Nel Hydrogen 2018)

The water flow rates required for the hydrogen production process are very large, consisting of the added water for the electrolyser and scrubbing water for the gas scrubber. The scrubbing water contains relatively low amount of impurities after the scrubbing. Thus, it could be applied to fulfill water requirements in other parts of the process and probably recycled in scrubbing. In the original electrolyser design by Nel Hydrogen (2017), it is applied to provide the fresh water added to the electrolyte mix. The utilization of scrubbing water should be further examined as the flow rate is very high equaling to 4 337,9 t/hr.

In general, the power and material (fresh water and electrolyte) requirements for hydrogen production in this scale are substantially large especially considering that only renewable electricity would be applied. Thus, hydrogen from other sources and/or electricity from the grid should be considered. Other possible hydrogen sources include industrial side streams and hydrogen from syngas.

Table 5.3. Key input and output figures for the hydrogen production process.

Parameter	**Value**	**Unit**
Produced H_2	5,07	t/hr
Produced O_2	40,1	t/hr
Electrolyte mix flow rate	207 273,6	t/hr
Makeup water flow rate	53,6	t/hr
Power consumption	217	MW

5.3 Methanol synthesis and distillation

Key input and output figures for the methanol synthesis process are introduced in Table 5.4 and the extracted stream data from Aspen is introduced in Appendix 3.

Table 5.4. Key input and output figures for the methanol synthesis process.

Parameter	**Value**	**Unit**
Crude methanol production rate	35 043,3	kg/hr
CO_2 input flow rate	39 721,4	kg/hr
H_2 input flow rate	5 066,5	kg/hr
Reactor temperature	250	^oC
Reactor pressure	50	bar
Recycle to feed ratio	3,86	mol/mol
H_2:CO_2 ratio (feed/reactor inlet)	2,74/2,99	mol/mol
Reactor heat generation	7,3	MW
Required electricity load	2,96	MW

The electricity load for methanol synthesis phase consists of the power consumption in the hydrogen feed compressor and the recycle stream compressor.

Considering the error analysis presented in chapter 4.4, the heat generation in the reactor (123,53 kJ/kg) implies the largest difference, being lower than the value (131,27 kJ/kg) achieved from the reported data by Kiss et al. (2016). This is primarily explained by the non-reactants, nitrogen and oxygen, in the reactor inlet stream which are not participating in the reactions inducing the heat generation. When not considering nitrogen and oxygen, the value is more relevant equaling to 128,4 kJ/kg.

Key input and output figures for the distillation process are introduced in Table 5.5.

Table 5.5. Key input and output figures for the distillation process.

Parameter	**Value**	**Unit**
Methanol production	21,25	t/hr
Methanol purity	99,6	%
Steam input flow rate	30	t/hr
Water output flow rate (first / second column)	9,9/ 32,5	t/hr
Reboiler heat duty (first column)	11 961,1	kW
Condenser heat duty (first / second column)	-2 176,9 / -21 697,2	kW
CO_2 feed per produced methanol	1,87	kg/kg
H_2 feed per produced methanol	0,24	kg/kg
Carbon conversion (methanol/CO_2)	0,757	mol/mol
Waste water production	42,4	t/hr

Most of the impurities in the produced methanol stream consist of dissolved CO_2. The rest are the minor amount of remaining moisture and traces of H_2, CO, N_2 and O_2. The composition of the produced methanol stream is introduced in Table 5.6.

The carbon conversion rate is substantially low compared to previous studies. In addition, the CO_2 and H_2 feeds per product are relatively high. (Kiss et al. 2016) This is primarily explained by the high purge rate due to the Aspen convergence method and the considered configuration in which the purges are combusted to produce heat. The heat from the combustion is exploited in the heat integration (for instance, covering the heat requirement for producing steam to the last distillation column) and produced excess heat could be exploited in power generation.
The conversion values could be enhanced applying a different convergence method and excluding the purge combustion. However, the heat source for steam generation should be then fulfilled in other means.

The distillation columns produce large waste water flows at 100 ºC temperature containing 184 ppm of methanol. These streams could be applied in heating purposes elsewhere in the process. For instance, preheating of the reactor feed could be a potential option to exploit the heat in these streams.

Table 5.6. Composition of the produced methanol.

Component	Mass fraction
CH_3OH	0,9958
CO_2	0,00413
H_2O	0,000113
H_2, CO, N_2, O_2	$1\text{-}3 * 10^{-6}$

5.4 Process optimization

Various released side products together with similar requirements elsewhere in the process provide possibilities for process optimization through connecting these streams. Major share of these streams are steam and liquid water streams of considerable flow rates. Some of them are applied for heat transfer purposes. Thus, finding the optimal configuration to for process water network is highly advantageous for process efficiency but is excluded in this study.

The pure oxygen stream released from hydrogen production is approximately three times larger than the oxygen requirement for the calciner in the CO_2 extraction phase. Thus, high costs induced by expensive air separation units or purchasing of exterior oxygen may be avoided by combining these streams. Additionally, the nitrogen resulting in the synthesis feed stream could be neglected if high purity oxygen from electrolysis would be exploited in combustion in the calciner. The excess oxygen surpassing the requirements of the calciner is a valuable side product applicable in various industrial processes and/or could be applied in the combustion of purges in the synthesis/distillation phase. The amount of excess oxygen may be attained from the difference of the flow rates of the produced and required oxygen flow rates and equals to 26 654,9 kg/hr.

The model includes several significant heat loads both consuming and producing heat. Thus, a heat integration analysis is conducted with the Aspen Energy Analyzer to find the optimal configuration considering the heat streams in the whole process. The analysis tool is applied in two parts (CO_2 extraction and synthesis together with distillation) as separate to avoid excessively complicated configurations. The results from the energy analysis are presented in Table 5.7.

Table 5.7. Energy analysis results.

Load	**Value**
Heating utilities (synthesis and distillation), original	45,6 MW
Heating utilities (synthesis and distillation), after analysis	0 MW
Cooling utilities (synthesis and distillation), original	102,5 MW
Cooling utilities (synthesis and distillation), after analysis	26,8 MW
Heating utilities (CO_2 extraction), original	14,7 MW
Heating utilities (CO_2 extraction), after analysis	0 MW
Cooling utilities (CO_2 extraction), original	16,1 MW
Cooling utilities (CO_2 extraction), after analysis	1,5 MW
Total savings (synthesis and distillation)	81,9 %
Total savings (CO_2 extraction)	95,2 %

As seen in the results, the system is thermally self-sufficient and no external heating is required (if not considering the CH_4 combusted in the calciner) with an optimized heat integration. However, some cooling is required and considered as losses rejecting heat to the environment. The utilization of the excess heat should be examined. For instance, heating of the large electrolyte mix flow in hydrogen production (at 80 ^oC) is excluded in the analysis.

5.5 Power consumption

The entire process includes notable electricity loads. Hydrogen production distinctly accounts for the largest share considering electricity consumption. The pumping of processed streams is excluded in the calculations. Additionally, the compressor inputs in the model assume 100 % isentropic efficiency. Thus, an additional electricity load induced by the pumping and losses in compression should be considered in actual design. The shares of electricity consumption in different parts of the process are introduced in Table 5.8.

Table 5.8. Electricity loads in different parts of the process.

Process block	**Electricity load, [MW]**	**Share of total electricity load**
Carbon dioxide extraction	8,84	3,9 %
Hydrogen production	217	94,8 %
Methanol synthesis	2,96	1,3 %
Distillation	0	0 %

The distinctly largest electricity load is induced by the hydrogen production phase. Water electrolysis equipment are typical applications for exploiting renewable electricity. In this scale, the electricity load is substantially large and would require immoderate electricity production considering average renewable resources. Thus, dependence on electricity from the grid or hydrogen feedstocks from other sources should be examined. Considering only methanol synthesis, the consumed electricity per ton of product seems to be reasonable equaling to 139 kWh/ton of methanol.

5.6 Summary of plant performance

This section provides a summary of the results for plant performance focusing on viewpoints on energy and material consumption and their efficiencies.

5.6.1 Material consumption

The mass balance of the entire process is defined comparing the inputs and outputs of the system as there is no accumulation of materials in the process. Exclusively, the material streams contributing to the product streams are considered and other operational streams are excluded from the material efficiency calculations. Thus, the streams considered as inputs are:

- carbon dioxide from air
- methane and oxygen for the calciner in CO_2 extraction
- water added in the electrolysis

and the streams considered as outputs are:

- methanol
- oxygen from electrolysis

Figure 5.1 presents an illustrated definition for the mass balance boundaries and the flow rates of the mentioned streams are introduced in Table 5.9.

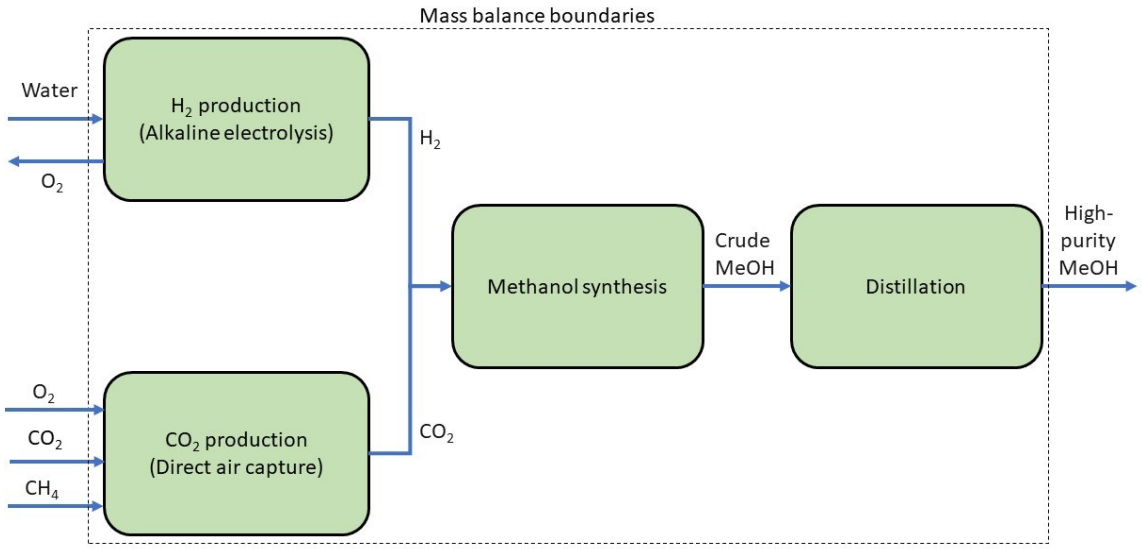

Figure 5.1. Illustrated definition for the considered mass balance boundaries.

Table 5.9. Flow rates in the mass balance.

Material	**Mass flow rate, [kg/hr]**
CO_2	29 526,4
Water	53 640
$O_{2,in}$	12 856
CH_4	3 034,6
Methanol	21 250
$O_{2,out}$	40 102,6
Losses	37 704,4

The primary output streams (methanol and oxygen) contribute to 61,9 % of the inputs. Considering only methanol, the ratio equals to 21,5 %. The losses in mass balance equal to 37 704,4 kg/hr, contributing to 38,1 % of the total mass flow of inputs. The losses consist of:

- purge in the recycle loop in methanol synthesis
- unreacted gases released as purge in the first distillation column
- water production in synthesis and released in the distillation columns
- water production in the combustion of methane in the calciner

The largest material requirements consist of water makeup for water electrolysis and methane fed to the calciner in the CO_2 extraction process if the required oxygen is considered to be fulfilled by the oxygen produced in the electrolysis. A major share of the other (operational) material loads in the process may be fulfilled by circulating the processed streams, as well. The degradation of potassium hydroxide acting as the sorbent in CO_2 capture and electrolyte in the hydrogen production as well as the degradation of the methanol synthesis catalyst induce a demand for replacing them at an adequate rate. This should be considered in the actual process design but is excluded in this study.

The mass balance could be examined considering different process phases as separate, as well. Table 5.10 describes the inputs and outputs together with the conversion ratios for mass balance of each process phase.

Table 5.10. Mass balance inputs, outputs and conversion ratios for different process steps.

Process phase	**Input(s)**	**Output(s)**	**Conversion ratio (output(s) / input(s))**
CO_2 extraction	CO_2 from air CH_4 O_2	CO_2	87,5 %
H_2 production	Water	H_2 O_2	84,2 %
Methanol synthesis	CO_2 H_2	Crude methanol	78,2 %
Distillation	Crude methanol	High purity methanol	60,6 %

In CO_2 extraction, the losses are mostly water produced in the consumption of methane. In H_2 production, the moisture resulting in the H_2 stream from the electrolyser contributes for the losses. The large purge ratio and water production in the synthesis reactions are primary reasons for losses in methanol synthesis and distillation phases.

Carbon conversion rate describes the molar conversion of inputs (carbon dioxide and methane) to outputs (methanol) containing carbon. The amount of CO_2 is determined to equal with the amount of CO_2 captured in the air contactor in the extraction phase to correlate with the carbon conversion efficiency of the entire plant. Thus, the amount of CO_2 equals to the molar amount of CO_2 in the stream "AIR-IN" diminished with the molar amount of CO_2 in the stream "AIR-OUT". The value may be defined by the following equation:

$$R_{CC} = \frac{moles_{CH3OH}}{moles_{CO2,CH4}} \quad \text{(Eq. 5.1)}$$

Thus, the carbon conversion rate of the entire process equals to 0,767. Similarly to the carbon conversion value determined in chapter 5.3, the relatively low value may be primarily explained by the high purge rate in the synthesis process.

5.6.2 Energy consumption

The total amount of energy consumed in the methanol production process compared to the energy released in its combustion defines the energy efficiency of the entire process design. The energy released in the combustion is defined by the lower heating value (LHV) of the combusted component. LHV for methanol is 19,9 MJ/kg and LHV for methane is 50,0 MJ/kg. (The Engineering ToolBox)

The total amount of consumed energy consists of electricity consumption in various parts of the process and methane fed to the calciner in CO_2 extraction. Energy loads considered as outputs are methanol (LHV basis), cooling utilities and other losses. Different shares in the energy efficiency calculations are introduced in Table 5.11.

The energy consumption is calculated considering the heat integration system determined after applying Aspen Energy Analyzer for the model. As seen in the energy analysis results introduced in chapter 5.4, all the heat loads in the process could be covered with optimized heat integration. However, some cooling loads are resulting still after the optimization as reject heat to the environment and considered as losses. The value for the total cooling load is determined from the values obtained after the energy analysis.

Table 5.11. Shares in the energy efficiency calculations.

Source	**Energy load, [MW]**
$\sum P_{elec}$	229
CH_4	42,4
Methanol	117
$\sum P_{cooling}$	28,3
Other losses	126,1

The consumed energy per produced methanol equals to 12,8 MWh/ton of methanol. Considering electricity load exclusively, the value equals to 10,8 MWh/ton of methanol. Comparing to previous studies, the energy consumption values seem to be reasonable considering the configuration of the plant that covers the whole process including CO_2 extraction and hydrogen production. A major share of the electricity load is induced by hydrogen production. Other process configurations such as feedstocks from other sources would have a large impact on the energy consumption values. A comparison between this and other studies is provided in Table 5.12.

Table 5.12. Comparison of key energy consumption values.

Parameter	This study	(Mignard et al. 2003)	(Specht et al. 1998)	(Sakamoto, Zhou 2000)	(Bellotti et al. 2017)	MeOH from biomass (Galindo Cifre, Badr 2007)
Electricity consumption, [MWh/ton of MeOH]	10,8	9,2	12,0	10	10,9	7
Energy conversion efficiency	43,1 %	18,4 – 23 %	17,6 %	21 %	45,6 %	25 %

The comparison of energy consumption between different studies is challenging as the reported values include different loads depending on the research in question. However, the comparison provides a view on the differences between the values from different process configurations. The study from Bellotti et al. (2017) is based on a largely similar configuration but where CO_2 is extracted from the flue gases of a coal power plant and hydrogen is produced via PEM electrolysis. The study by Galindo Cifre and Badr (2007) focused on methanol production via biomass gasification and provided lowest values considering electricity consumption even though the electricity load for water electrolysis was included. The other three studies investigated conventional CO_2 hydrogenation to methanol –plants where CO_2 was captured from flue gases. Specht et al. (1998) and Sakamoto and Zhou (2000) also included the delivery of CO_2 in their calculations. In general, the novel design in this study seems to be competitive with other methanol production processes considering both electricity consumption and energy conversion efficiency.

Plant overall efficiency describes the process comparing its inputs and outputs. The input value equals to the amount of consumed energy consisting of the same components as considered in the energy efficiency calculations previously introduced in this chapter but excluding the cooling loads. The outputs are determined for methanol exclusively applying both lower heating value (LHV) and higher heating value (HHV) as a basis. LHV basis represents the efficiency considering the produced methanol to be exploited as a fuel and HHV basis represents the efficiency of methanol exploited as a chemical feedstock. The higher heating value for methanol is 23,0 MJ/kg. (The Engineering ToolBox) The values are obtained by the following equations:

$$\eta_{LHV} = \frac{LHV_{methanol} * mass\ flow_{methanol}}{E_{in}} \quad \text{(Eq. 5.2)}$$

$$\eta_{HHV} = \frac{HHV_{methanol} * mass\ flow_{methanol}}{E_{in}} \quad \text{(Eq. 5.3)}$$

The plant overall efficiency with LHV basis equals to 43,1 % and with HHV basis to 50,0 %.

5.7 Suggestions

PEM and SOEC electrolysers provide interesting options for the conventional alkaline electrolysers. The more compact design considering PEM electrolysers and the electrical energy efficiency considering SOEC electrolysers (when enough thermal energy is available) are preferred compared to alkaline processes. In addition, the potential in dynamic operation of PEM electrolysers is an advantage in processes where fluctuating renewable electricity is applied. However, PEM electrolysis is largely cost-intensive and both PEM and SOEC electrolysers would require more research and development to reach higher feasibility in industrial operation.

Various catalysts have been examined for methanol synthesis that overcome the most applied $Cu/ZnO/Al_2O_3$ -compound and the Cu/Zn/Al/Zr compound considered in this study. The main advantages of the novel catalysts are increasing the selectivity for CO_2 hydrogenation reaction and methanol yields. Further research and development of the operation of the novel catalysts would provide possibilities to increase the efficiency of the system and investigate their feasibility.

Further process optimization is suggested to reduce the energy and material requirements per produced methanol. In this study, more profound optimization of water flows (integration and flow rates) is excluded and leaves a large potential for further research. The large amount of purge in the synthesis phase induces excess losses considering feed conversion ratios compared to typical designs from previous studies. This should be optimized in the model design, as well. However, the proposed design in this study for combustion of purges removes all the heating requirements in the process.

6 Conclusion

This thesis examined the production of methanol via carbon dioxide hydrogenation. Methanol is a chemical that is primarily applied as a fuel or base chemical in chemical industry. It may be produced from several feedstocks and in various pathways. Renewable methanol production is one of the most promising methods in sustainable power-to-liquids/power-to-fuel scenarios.

For this thesis, a simulation model was built in Aspen Plus software to investigate the whole methanol production process from CO_2 capture from ambient air and hydrogen production via water electrolysis to distilled high purity methanol. The discussed methods resulted in a novel process configuration considering the complete plant design.

The considered scale (170 000 tons of methanol per year) results in high material and electricity demand, posing a question about potentially suitable locations especially if renewable electricity would be exclusively applied. This is primarily due to the substantially large power and material requirements (217 MW of electricity and 53 640 kg/hr of fresh water for the electrolyser and even more as scrubbing water) in the hydrogen production. Thus, at least partial hydrogen feedstock from other sources and/or electricity from the grid should be considered. Apart from hydrogen production, the process seems to be reasonable considering requirements per product.

The CO_2 capture process from ambient air provides an interesting possibility to reduce the amount of CO_2 in the atmosphere and dependence on conventional fossil fuel –based methods in CO_2 extraction especially if renewable-based methane is considered in heating of the calciner. The process seems to be feasible considering the energy requirements per produced CO_2. After the energy analysis, all the heating loads and most of the cooling loads could be covered with optimized heat integration. However, large water flows are required for this process phase, as well.

Process optimization plays an important role as the considered plant configuration includes several large material and heat loads. A heat integration analysis was performed with Aspen Energy Analyzer tool. As seen in the results, all of the heating requirements in the entire process could be covered with optimized heat integration. However, some cooling requirements still remain rejecting heat to the environment. The largest material requirements consist of water/steam streams applied in various stages of the process. In addition, the high purity oxygen produced in water electrolysis and applied in methane combustion in the calciner (and/or combustion of purge streams in methanol synthesis) provide interesting options for process optimization. Further examination on these is suggested.

In general, a plant of a smaller scale would be more feasible as the material and electricity requirements in this design are relatively large. The most potential options to increase the plant feasibility would probably be to decrease the overall scale and to apply possible available hydrogen feedstocks from e.g. industrial side streams. However, the economical feasibility of the CO_2 capture process decreases in relation to the scale. Further examination is suggested related to the plant scale and feedstocks from other sources.

Overall, the novel configuration considered in this study seems to be competitive with conventional methanol production methods considering its efficiency. The obtained plant efficiency values seem to be reasonable even though the power requirements are high and a

relatively large share of the feeds for the synthesis are purged. However, the carbon conversion rate considering the whole process remains relatively low due to the large amount of purges. The values could be further improved as the research leaves a large potential in optimization of the material streams and their flow rates and thus enhancing the efficiency of the plant.

7 References

AspenTech. *Aspen Plus*. Available at: < https://www.aspentech.com/en/products/engineering/aspen-plus> [Accessed: 19.11.2018]

Baltrusaitis, J., Luyben, W. L. 2015. *Methane Conversion to Syngas for Gas-to-Liquids (GTL): Is Sustainable CO_2 Reuse via Dry Methane Reforming (DMR) Cost Competitive with SMR and ATR Processes?*. ACS Sustainable Chemistry & Engineering, 3/2015, pp. 2100-2111. Available at: <https://pubs.acs.org/doi/pdf/10.1021/acssuschemeng.5b00368>

Barbir, F. 2005. *PEM electrolysis for production of hydrogen from renewable energy sources.* Solar Energy, 78/2005, pp. 661-669. Available at: <https://ac.els-cdn.com/S0038092X04002464/1-s2.0-S0038092X04002464-main.pdf?_tid=8eb47ed4-de74-11e7-ab6c-00000aacb361&acdnat=1512997965_bf6c9924b0366aaad60366b2cc21ab41>

Bellotti, D., Rivarolo, M., Magistri, L., Massardo, A. F. 2017. *Feasibility study of methanol production plant from hydrogen and captured carbon dioxide*. Journal of CO_2 Utilization, 21/2017, pp. 132-138. Available at: < https://reader.elsevier.com/reader/sd/pii/S2212982017302007?token=D3E0BD597C7A0CC5B5EB500540A64F81BAE041DA740A45A56C4B29FE083FE7B9C89A7550EBCCB7B73926A9F117E3FB2C>

DOE - U.S. Department of Energy. *Hydrogen Production and Distribution*. Available at: <https://afdc.energy.gov/fuels/hydrogen_production.html> [Accessed: 14.11.2018]

EPA - United States Environmental Protection Agency. *Overview of Greenhouse Gases - Carbon Dioxide Emissions*. Available at: <https://www.epa.gov/ghgemissions/overview-greenhouse-gases#carbon-dioxide> [Accessed: 6.11.2018]

Frilund, C. 2016. *CO_2 Hydrogenation to Methanol.* [online]. M.Sc. Thesis. Aalto University School of Chemical Technology. Espoo. 121 p. [referenced 11.12.2017] Available at: <https://aaltodoc.aalto.fi/bitstream/handle/123456789/19938/master_Frilund_Christian_2016.pdf?sequence=1&isAllowed=y>

Galindo Cifre, P., Badr, O. 2007. *Renewable hydrogen utilisation for the production of methanol.* Energy Conversion and Management, 48/2007, pp. 519-527. Available at: <https://ac-els-cdn-com.libproxy.aalto.fi/S0196890406002020/1-s2.0-S0196890406002020-main.pdf?_tid=6a6a40fb-4ecb-4684-a264-61256e66064b&acdnat=1534762220_6dbaf29676759c93e91d4b0739ccc732>

Gesser, H. D., Hunter, N. R., Prakash, C. B. 1985. *The Direct Conversion of Methane to Methanol by Controlled Oxidation*. Chemical Reviews, 85/1985, nr. 4, pp. 235-244. Available at: <https://pubs.acs.org/doi/pdf/10.1021/cr00068a001>

Goeppert, A., Czaun, M., May, R. B., Prakash, G. K. S., Olah, G. A., Narayanan, S. R. 2012. *Air as the renewable carbon source of the future: and overview of CO_2 capture from the atmosphere.*

Energy & Environmental Science, 5/2012, pp. 7833-7853. Available at: <http://pubs.rsc.org.libproxy.aalto.fi/en/content/articlepdf/2012/ee/c2ee21586a>

Goeppert, A., Czaun, M., May, R. B., Prakash, G. K. S., Olah, G. A., Narayanan, S. R. 2011. *Carbon Dioxide Capture from the Air Using a Polyamine Based Regenerable Solid Adsorbent.* Journal of the American Chemical Society, 135/2011, pp. 20164-20167. Available at: <https://pubs-acs-org.libproxy.aalto.fi/doi/pdf/10.1021/ja2100005>

Han, B., Yang, Y., Xu, Y., Etim, U. J., Qiao, K., Xu, B., Yan, Z. 2016. *A review of the direct oxidation of methane to methanol.* Chinese Journal of Catalysis, 37/2016, pp. 1206-1215. Available at: <https://ac.els-cdn.com/S187220671561097X/1-s2.0-S187220671561097X-main.pdf?_tid=spdf-cb26f174-dfc1-4e9a-8d25-6fdf9600b9d1&acdnat=1519664085_ccca3ace94f174da48797ffd58c68e8e>

Holladay, J. D., Hu, J., King, D. L., Wang, Y. 2009. *An overview of hydrogen production technologies.* Catalysis Today, 139/2009, pp. 244-260. Available at: <https://ac-els-cdn-com.libproxy.aalto.fi/S0920586108004100/1-s2.0-S0920586108004100-main.pdf?_tid=f61a6286-342d-4e22-b3a3-6c7e5367813d&acdnat=1534770743_16e8ea24b5d0e3f35b51c6d6719deac8>

Hydrocarbons Technology: *Neste Oil Porvoo Refinery Diesel Project, Porvoo.* Available at: <https://www.hydrocarbons-technology.com/projects/fortum/> [Accessed: 24.9.2018]

Keith, D. W., Holmes, G., St. Angelo, D., Heidel, K. 2018. *A Process for Capturing CO_2 from the Atmosphere.* Joule, 2/2018, pp. 1-22. Available at: <https://www.cell.com/joule/pdf/S2542-4351(18)30225-3.pdf>

Kiss, A. A., Pragt, J. J., Vos, H. J., Bargeman, G., de Groot, M. T. 2016. *Novel efficient process for methanol synthesis by CO_2 hydrogenation.* Chemical Engineering Journal, 284/2016, pp. 260-269. Available at: <https://ac.els-cdn.com/S1385894715011833/1-s2.0-S1385894715011833-main.pdf?_tid=11b14841-3776-4374-8cf7-15cf9bd7246e&acdnat=1537863946_96f07d9b4ec97a9d8b4e81d942c6bf27>

Kondratenko, E. V., Peppel, T., Seeburg, D., Kondratenko, V. A., Kalevaru, N., Martin, A., Wohlrab, S. 2017. *Methane conversion into different hydrocarbons or oxygenates: current status and future perspectives in catalyst development and reactor operation.* Catalysis Science & Technology, 7/2017, pp. 366-381. Available at: <http://pubs.rsc.org/en/content/articlepdf/2017/cy/c6cy01879c>

Koponen, J. 2015. *Review of water electrolysis technologies and design of renewable hydrogen production systems.* [online]. M.Sc. Thesis. Lappeenranta University of Technology, School of Energy Systems. Lappeenranta. 87 p. [referenced 22.12.2017] Available at: <https://www.doria.fi/bitstream/handle/10024/104326/MScThesis_JKK.pdf>

Kothandaraman, J., Goeppert, A., Czaun, M., Olah, G. A., Prakash, G. K. S. 2015. *Conversion of CO_2 from Air into Methanol Using a Polyamine and a Homogeneous Ruthenium Catalyst.*

Journal of the American Chemical Society, 138/2016, pp. 778-781. Available at: <https://pubs-acs-org.libproxy.aalto.fi/doi/pdf/10.1021/jacs.5b12354>

Lackner, K. S. 2009. *Capture of carbon dioxide from ambient air.* The European Physical Journal Special Topics, 176/2009, pp. 93-106. Available at: <https://link.springer.com/content/pdf/10.1140%2Fepjst%2Fe2009-01150-3.pdf>

Lee, S., Sardesai, A. 2005. *Liquid phase methanol and dimethyl ether synthesis from syngas.* Topics in Catalysis, 32/2005, nro. 3-4, pp. 197-207. Available at: <https://link-springer-com.libproxy.aalto.fi/content/pdf/10.1007%2Fs11244-005-2891-8.pdf>

Leung, D. Y. C., Caramanna, G., Maroto-Valer, M. M. 2014. *An overview of current status of carbon dioxide capture and storage technologies.* Renewable and Sustainable Energy Reviews, 39/2014, pp. 426-443. Available at: <https://ac.els-cdn.com/S1364032114005450/1-s2.0-S1364032114005450-main.pdf?_tid=36c8525b-51a5-4bf2-b5df-44b72e4daf56&acdnat=1522079659_9c1c687f4f666397fd49fc34e8b216df>

The Linde Group - Linde Engineering 2018. *Isothermal reactor.* Available at: <https://www.linde-engineering.com/en/process_plants/hydrogen_and_synthesis_gas_plants/gas_generation/isothermal_reactor/index.html> [Accessed 24.8.2018]

Mansilla, C., Dautremont, S., Shoai Tehrani, B., Cotin, G., Avril, S., Burkhalter, E. 2011. *Reducing the hydrogen production cost by operating alkaline electrolysis as a discontinuous process in the French market context.* International Journal of Hydrogen Energy, 36/2011, pp. 6407-6413. Available at: <https://ac.els-cdn.com/S0360319911005921/1-s2.0-S0360319911005921-main.pdf?_tid=5ae4b4e6-e6ff-11e7-8af7-00000aab0f6b&acdnat=1513937196_3362be08b405f34baacfb27aa5b44382>

Mergel, J., Carmo, M., Fritz, D. 2013. *Status on Technologies for Hydrogen Production by Water Electrolysis.* Transition to Renewable Energy Systems, 1st Edition, 937 p. Wiley-VCH Verlag GmbH & Co. ISBN: 978-3-527-33239-7 Available at: <https://s3.amazonaws.com/academia.edu.documents/48594644/Transition_to_Renewable_Energy.pdf?AWSAccessKeyId=AKIAIWOWYYGZ2Y53UL3A&Expires=1513242396&Signature=yG64sWp%2B3jZStFm6Y2R%2BwER45aE%3D&response-content-disposition=inline%3B%20filename%3DTransition_to_Renewable_Energy_Systems.pdf#page=449>

Meunier, N., Laribi, S., Dubois, L., Thomas, D., de Weireld, G. 2014. *CO_2 capture in cement production and re-use: first step for the optimization of the overall process.* Energy Procedia, 63/2014, pp. 6492-6503. Available at: <https://ac.els-cdn.com/S1876610214025004/1-s2.0-S1876610214025004-main.pdf?_tid=0c42d610-f9e4-40bf-a330-510d743997c4&acdnat=1522080820_f7bc14c434454aa0facc8ee99f4a20e1>

Mignard, D., Sahibzada, M., Duthie, J. M., Whittington H. W. 2003. *Methanol synthesis from flue-gas CO_2 and renewable electricity: a feasibility study*. International Journal of Hydrogen Energy, 28/2003, pp. 455-464. Available at: < https://ac.els-cdn.com/S0360319902000824/1-

s2.0-S0360319902000824-main.pdf?_tid=5510bd95-2bac-41b3-9e35-cb890eab93c6&acdnat=1542638978_cecd28659783d19d4fc7443028fb6932>

Nel Hydrogen 2018. *Constructing the world's largest electrolyzer manufacturing plant.* Available at: <https://nelhydrogen.com/press-release/constructing-the-worlds-largest-electrolyzer-manufacturing-plant/>

Nel Hydrogen 2017. *Nel Hydrogen Electrolyser - The world's most efficient and reliable electrolyser.* Available at: <http://nelhydrogen.com/assets/uploads/2017/01/Nel_Electrolyser_brochure.pdf>

Ni, M., Leung, M. K. H., Leung, D. Y. C. 2008. *Technological development of hydrogen production by solid oxide electrolyzer cell (SOEC).* International Journal of Hydrogen Energy, 33/2008, pp. 2337-2354. Available at: <https://ac.els-cdn.com/S0360319908002255/1-s2.0-S0360319908002255-main.pdf?_tid=fb01f71e-df29-11e7-8119-00000aacb35d&acdnat=1513075886_f252f7c13ad65aabe4af7501550f86f9>

Olah, G.A. 2005. *Beyond Oil and Gas: The Methanol Economy.* Angewandte Chemie International Edition, 44/2005, pp. 2636-2639. Available at: <http://onlinelibrary.wiley.com/doi/10.1002/anie.200462121/epdf>

Ott, J., Gronemann, V., Pontzen, F., Fiedler, E., Grossmann, G., Kersebohm, D. B., Weiss, G., Witte, C. 2012. *Ullmann's Encyclopedia of Industrial Chemistry - Methanol*. Wiley-VCH Verlag GmbH & Co. KGaA, Weinheim. ISBN: 978-3-527-30673-2. Available at: <http://www.ugr.es/~tep028/pqi/descargas/Industria%20quimica%20organica/tema_1/documentos_adicionales/a16_465_metanol.pdf>

Rahimpour, M. R. 2008. *A two-stage catalyst bed concept for conversion of carbon dioxide into methanol.* Fuel Processing Technology, 89/2008, pp. 556-566. Available at: <https://ac.els-cdn.com/S0378382007002226/1-s2.0-S0378382007002226-main.pdf?_tid=c8382a2c-e17e-11e7-b334-00000aacb35f&acdnat=1513332210_581e8ac12a8159214caf003d22b755a5>

Rahimpour, M. R., Alizadehhesari, K. 2008. *A Novel Fluidized-bed Membrane Dual-type Reactor Concept for Methanol Synthesis.* Chemical Engineering Technology, 31/2008, nr. 31, pp. 1775-1789. Available at: <https://onlinelibrary.wiley.com/doi/epdf/10.1002/ceat.200800375>

Sadeghi, J., Ahangar, M. 2012. *The Study of Methanol Separation Columns Control.* Oriental Journal of Chemistry, 28/2012, nr. 1, pp. 229-235. Available at: <http://orientjchem.org/dnload/Jafar-Sadeghi26sup-and-Mansureh-Ahangar26sup-/OJCV028I01P229-235.pdf>

Sakamoto, Y., Zhou, W. 2000. *Energy analysis of a CO_2 recycling system*. International Journal of energy Research, vol. 24, iss. 6, pp. 549-559.

Sanz-Pérez, E. S., Murdock, C. R., Didas, S. A., Jones, C. W. 2016. *Direct Capture of CO_2 from Ambient Air.* Chemical Reviews, 116/2016, pp. 11840-11876. Available at: <https://pubs.acs.org/doi/pdf/10.1021/acs.chemrev.6b00173>

Shekhah, O., Belmabkhout, Y., Chen, Z., Guillerm, V., Cairns, A., Adil, K., Eddaoudi, M. 2014. *Made-to-order metal-organic frameworks for trace carbon dioxide removal and air capture.* Nature Communications, 5:4228. Available at: <https://www.nature.com/articles/ncomms5228.pdf>

da Silva, M. J. 2016. *Synthesis of methanol from methane: Challenges and advances on the multi-step (syngas) and one-step routes (DMTM).* Fuel Processing Technology, 145/2016, pp. 42-61. Available at: <https://ac-els-cdn-com.libproxy.aalto.fi/S0378382016300224/1-s2.0-S0378382016300224-main.pdf?_tid=spdf-0881a1ed-c76d-4329-8132-cd7fcdd0dc9a&acdnat=1519907771_f6587ba9850a1828f51dc959e819658a>

Specht, M., Bandi, A., Elser, M., Staiss, F. 1998. *Comparison of CO_2 sources for the synthesis of renewable methanol*. In: Inui, T., Anpo, M., Izui, K., Yanagida, S., Yamaguchi, T. 1998. *Advances in chemical conversions for mitigating carbon dioxide*. Vol.114, pp. 363-367. Elsevier, Amsterdam, the Netherlands.

Studt, F., Sharafutdinov, I., Abild-Pedersen, F., Elkjaer, C. F., Hummelshoej, J. S., Dahl, S., Chorkendorff, I., Noerskov, J. K. 2014. *Discovery of a Ni-Ga catalyst for carbon dioxide reduction to methanol.* Nature Chemistry, 6/2014, pp. 320-324. Available at: <http://web.a.ebscohost.com/ehost/pdfviewer/pdfviewer?vid=1&sid=77c54260-8457-46ec-998b-62c9bfe8db7e%40sessionmgr4007>

Sun, J., Wang, F., Ma, T., Gao, H., Wu, P., Liu, L. 2012. *Energy and exergy analysis of a five-column methanol distillation scheme.* Energy, 45/2012, pp. 696-703. Available at: <https://ac.els-cdn.com/S0255270110001534/1-s2.0-S0255270110001534-main.pdf?_tid=spdf-bd6398a9-3710-4234-9548-073002c24289&acdnat=1519373448_1d63e2031d58179b104f8d34b156ec61>

The Engineering ToolBox: *Fuels - Higher and Lower Calorific Values*. Available at: <https://www.engineeringtoolbox.com/fuels-higher-calorific-values-d_169.html> [Accessed: 5.11.2018]

Tijm, P. J. A., Waller, F. J., Brown, D. M. 2001. *Methanol technology developments for the new millenium.* Applied Catalysis - A: General, 221/2001, pp. 275-282. Available at: <https://ac-els-cdn-com.libproxy.aalto.fi/S0926860X01008055/1-s2.0-S0926860X01008055-main.pdf?_tid=70fdea08-42c6-4ec3-9474-d880b47daedb&acdnat=1537536283_e141631a5f2460069a4086c56870ab05>

van der Ham, L. G. J., van den Berg, H., Benneker, A., Simmelink, G., Timmer, J., van Weerden, S. 2012. *Hydrogenation of Carbon Dioxide for Methanol Production.* Chemical Engineering Transactions, 29/2012, pp. 181-186. Available at: <https://ris.utwente.nl/ws/portalfiles/portal/6917464>

Wang, W., Wang, S., Ma, X., Gong, J. 2011. *Recent advances in catalytic hydrogenation of carbon dioxide.* Chemical Society Reviews, vol.40/2011, nr. 7, pp. 3703-3727. Available at: <http://pubs.rsc.org/en/content/articlepdf/2011/cs/c1cs15008a>

Wilhelm, D. J., Simbeck, D. R., Karp, A. D., Dickenson, R. L. 2001. *Syngas production for gas-to-liquids applications: technologies, issues and outlook*. Fuel Processing Technology, 71/2001, pp. 139-148. Available at: <https://ac.els-cdn.com/S0378382001001400/1-s2.0-S0378382001001400-main.pdf?_tid=2f5496ba-17c0-11e8-85ad-00000aab0f01&acdnat=1519297671_ca27b3a0a4c75702da90ef0282110c9d>

York, A. P. E., Xiao, T., Green, M. L. H. 2003. *Brief overview of the partial oxidation of methane to synthesis gas.* Topics in Catalysis, 22/2003, nr. 3-4, pp. 345-358. Available at: <https://link-springer-com.libproxy.aalto.fi/content/pdf/10.1023%2FA%3A1023552709642.pdf>

Zakaria, Z., Kamarudin, S. K. 2016. *Direct conversion technologies of methane to methanol: An overview.* Renewable and Sustainable Energy Reviews, 65/2016, pp. 250-261. Available at: <https://ac.els-cdn.com/S1364032116301940/1-s2.0-S1364032116301940-main.pdf?_tid=spdf-d9a6ad67-558f-4f6d-9e3c-d31c10ef0641&acdnat=1519812021_5bfcfe9d787dedf6fcbfd99f793ac2d0>

Zhang, J., Liang, S., Feng, X. 2010. *A novel multi-effect methanol distillation process.* Chemical Engineering and Processing, 49/2010, pp. 1031-1037. Available at: <https://ac.els-cdn.com/S0255270110001534/1-s2.0-S0255270110001534-main.pdf?_tid=spdf-bd6398a9-3710-4234-9548-073002c24289&acdnat=1519373448_1d63e2031d58179b104f8d34b156ec61>

Appendix

Appendix 1. Error analysis for determining the synthesis reaction rates.

The applied case is found on the last row (226).

Row	Status	CO2 hydr. rate	rWGS rate	Q kW	FEED kg/sec	N2 mass frac	O2 mass frac.	Q/ [feed-(N2,O2)] kJ/kg	Q/ feed Err.	METH yield Err.	CO2 conv. Err.	H2 conv. Err.	Total Err.	Rank
1	Warnings	0,081	0,081	-6515	69,726	0,0461	0,0532	-103,738557	-21 %	-10 %	10 %	17 %	14,68 %	217
2	OK	0,081	0,083	-6570,2	69,307	0,04674	0,05394	-105,413232	-20 %	-9 %	9 %	17 %	13,61 %	214
3	OK	0,081	0,085	-6620,5	68,866	0,04716	0,05443	-107,007287	-18 %	-8 %	7 %	17 %	12,74 %	208
4	Warnings	0,081	0,087	-6674,5	68,428	0,04751	0,05483	-108,661193	-17 %	-7 %	5 %	17 %	11,78 %	199
5	OK	0,081	0,089	-6745	67,913	0,04788	0,05525	-110,739577	-16 %	-6 %	4 %	13 %	9,89 %	179
6	OK	0,081	0,091	-6798,7	67,467	0,04819	0,05562	-112,442971	-14 %	-6 %	3 %	13 %	8,80 %	167
7	OK	0,081	0,093	-6846,4	67,035	0,0485	0,05597	-114,046935	-13 %	-5 %	1 %	13 %	7,90 %	155
8	Warnings	0,081	0,095	-6894,9	66,625	0,04879	0,05631	-115,641659	-12 %	-4 %	1 %	13 %	7,41 %	146
9	Warnings	0,081	0,097	-6942,8	66,211	0,04909	0,05666	-117,258372	-11 %	-3 %	3 %	13 %	7,31 %	144
10	Warnings	0,081	0,099	-7004,3	65,757	0,04943	0,05704	-119,209377	-9 %	-2 %	4 %	11 %	6,42 %	126
11	OK	0,081	0,101	-7067,6	65,289	0,04976	0,05744	-121,247895	-8 %	-1 %	5 %	7 %	5,23 %	89
12	OK	0,081	0,103	-7115,8	64,887	0,05007	0,05779	-122,922762	-6 %	0 %	7 %	7 %	4,97 %	81
13	OK	0,081	0,105	-7159,1	64,496	0,05037	0,05813	-124,51112	-5 %	1 %	8 %	7 %	5,30 %	94
14	Warnings	0,081	0,107	-7203,5	64,124	0,05065	0,05846	-126,097061	-4 %	2 %	10 %	7 %	5,65 %	109
15	Warnings	0,081	0,109	-7246,9	63,749	0,05095	0,0588	-127,691858	-3 %	3 %	12 %	7 %	5,99 %	117
16	Warnings	0,083	0,081	-6602,3	69,19	0,04697	0,05421	-106,163766	-19 %	-9 %	10 %	13 %	12,84 %	210
17	OK	0,083	0,083	-6646,1	68,77	0,04728	0,05456	-107,600236	-18 %	-8 %	8 %	15 %	12,28 %	204
18	Warnings	0,083	0,085	-6689,3	68,355	0,04757	0,0549	-109,033411	-17 %	-7 %	6 %	17 %	11,76 %	198
19	Warnings	0,083	0,087	-6761,1	67,844	0,04793	0,05531	-111,130029	-15 %	-6 %	5 %	13 %	9,91 %	180
20	OK	0,083	0,089	-6813,6	67,399	0,04824	0,05567	-112,817201	-14 %	-5 %	3 %	13 %	8,82 %	169
21	OK	0,083	0,091	-6861,2	66,967	0,04854	0,05603	-114,420342	-13 %	-5 %	1 %	13 %	7,91 %	158
22	Warnings	0,083	0,093	-6911,7	66,553	0,04884	0,05637	-116,063322	-12 %	-4 %	0 %	13 %	7,09 %	139
23	OK	0,083	0,095	-6977,8	66,07	0,04919	0,05677	-118,12903	-10 %	-3 %	1 %	9 %	5,82 %	115
24	OK	0,083	0,097	-7027,9	65,654	0,0495	0,05712	-119,819215	-9 %	-2 %	3 %	9 %	5,53 %	102
25	OK	0,083	0,099	-7072,5	65,251	0,0498	0,05747	-121,413075	-8 %	-1 %	5 %	9 %	5,47 %	101
26	Warnings	0,083	0,101	-7117,8	64,869	0,05008	0,0578	-122,994992	-6 %	0 %	6 %	9 %	5,41 %	98
27	Warnings	0,083	0,103	-7162,3	64,484	0,05038	0,05814	-124,593508	-5 %	1 %	8 %	9 %	5,76 %	113
28	Warnings	0,083	0,105	-7219,6	64,061	0,05071	0,05852	-126,517894	-4 %	2 %	9 %	7 %	5,36 %	97

Row Status	CO2 hydr. rate	rWGS rate	Q kW	FEED kg/sec	N2 mass frac	O2 mass frac.	Q/ [feed-(N2,O2)] kJ/kg	Q/ feed Err.	METH yield Err.	CO2 conv. Err.	H2 conv. Err.	Total Err.	Rank
29 Warnings	0,083	0,107	-7265,3	63,677	0,051	0,05886	-128,178698	-2 %	3 %	11 %	6 %	5,57 %	104
30 Warnings	0,083	0,109	-7310,6	63,304	0,0513	0,0592	-129,829808	-1 %	4 %	13 %	6 %	5,78 %	114
31 Warnings	0,085	0,081	-6669,7	68,668	0,04735	0,05464	-108,161601	-18 %	-8 %	9 %	14 %	11,98 %	202
32 OK	0,085	0,083	-6719,4	68,229	0,04765	0,055	-109,748575	-16 %	-7 %	7 %	14 %	11,12 %	192
33 Warnings	0,085	0,085	-6766,8	67,801	0,04795	0,05534	-111,301922	-15 %	-6 %	5 %	15 %	10,30 %	187
34 Warnings	0,085	0,087	-6823,2	67,35	0,04827	0,05571	-113,066341	-14 %	-5 %	4 %	14 %	9,11 %	172
35 Warnings	0,085	0,089	-6872,3	66,927	0,04857	0,05606	-114,682542	-13 %	-4 %	2 %	14 %	8,18 %	161
36 OK	0,085	0,091	-6940	66,436	0,04892	0,05646	-116,767451	-11 %	-3 %	1 %	10 %	6,33 %	123
37 OK	0,085	0,093	-6989,7	66,016	0,04923	0,05682	-118,440542	-10 %	-3 %	1 %	10 %	5,73 %	112
38 OK	0,085	0,095	-7035,1	65,606	0,04953	0,05717	-120,04014	-9 %	-2 %	3 %	10 %	5,64 %	108
39 Warnings	0,085	0,097	-7094,2	65,176	0,04985	0,05753	-121,94257	-7 %	-1 %	4 %	7 %	4,82 %	74
40 Warnings	0,085	0,099	-7145,4	64,763	0,05016	0,05789	-123,698204	-6 %	0 %	6 %	6 %	4,49 %	60
41 OK	0,085	0,101	-7176	64,395	0,05044	0,05822	-125,022729	-5 %	1 %	7 %	8 %	5,23 %	88
42 Warnings	0,085	0,103	-7221,1	64,027	0,05073	0,05855	-126,619942	-4 %	2 %	9 %	8 %	5,73 %	111
43 OK	0,085	0,105	-7293	63,566	0,05109	0,05896	-128,918254	-2 %	3 %	10 %	3 %	4,52 %	61
44 OK	0,085	0,107	-7337	63,192	0,05139	0,05931	-130,558238	-1 %	4 %	12 %	3 %	4,67 %	69
45 OK	0,085	0,109	-7377,6	62,825	0,05168	0,05965	-132,141273	1 %	5 %	13 %	3 %	5,34 %	95
46 Warnings	0,087	0,081	-6741,5	68,123	0,04772	0,05507	-110,297899	-16 %	-7 %	8 %	13 %	10,81 %	190
47 OK	0,087	0,083	-6790,5	67,7	0,04802	0,05542	-111,875043	-15 %	-6 %	6 %	13 %	9,98 %	182
48 Warnings	0,087	0,085	-6829,8	67,294	0,04831	0,05575	-113,279393	-14 %	-5 %	4 %	15 %	9,41 %	177
49 OK	0,087	0,087	-6901,7	66,801	0,04866	0,05616	-115,413781	-12 %	-4 %	3 %	11 %	7,53 %	148
50 OK	0,087	0,089	-6951,9	66,376	0,04897	0,05651	-117,085026	-11 %	-3 %	1 %	11 %	6,45 %	127
51 OK	0,087	0,091	-7006,8	65,935	0,04929	0,05689	-118,892855	-9 %	-2 %	0 %	9 %	5,28 %	92
52 Warnings	0,087	0,093	-7054,7	65,533	0,04958	0,05722	-120,523374	-8 %	-1 %	2 %	9 %	5,16 %	86
53 OK	0,087	0,095	-7110,6	65,099	0,04991	0,0576	-122,383689	-7 %	-1 %	3 %	7 %	4,44 %	59
54 Warnings	0,087	0,097	-7152,6	64,714	0,0502	0,05794	-123,92662	-6 %	0 %	5 %	7 %	4,56 %	63
55 Warnings	0,087	0,099	-7191,9	64,353	0,05048	0,05826	-125,393319	-4 %	1 %	7 %	8 %	5,27 %	91
56 OK	0,087	0,101	-7258	63,892	0,05083	0,05866	-127,566096	-3 %	2 %	8 %	4 %	4,22 %	51

Row	Status	CO2 hydr. rate	rWGS rate	Q kW	FEED kg/sec	N2 mass frac	O2 mass frac.	Q/ [feed-(N2,O2)] kJ/kg	Q/ feed Err.	METH yield Err.	CO2 conv. Err.	H2 conv. Err.	Total Err.	Rank
57	OK	0,087	0,103	-7305,4	63,505	0,05114	0,05902	-129,277092	-2 %	3 %	10 %	3 %	4,28 %	55
58	Warnings	0,087	0,105	-7346,1	63,144	0,05142	0,05935	-130,831804	0 %	4 %	11 %	3 %	4,66 %	68
59	Warnings	0,087	0,107	-7392,2	62,774	0,05172	0,05969	-132,523401	1 %	5 %	13 %	3 %	5,29 %	93
60	Warnings	0,087	0,109	-7431,8	62,422	0,05201	0,06002	-134,077388	2 %	6 %	14 %	3 %	6,25 %	122
61	OK	0,089	0,081	-6828,1	67,568	0,0481	0,05551	-112,735146	-14 %	-6 %	7 %	10 %	9,25 %	176
62	Warnings	0,089	0,083	-6859,9	67,085	0,04845	0,05591	-114,172745	-13 %	-5 %	5 %	11 %	8,41 %	164
63	Warnings	0,089	0,085	-6912,4	66,744	0,0487	0,0562	-115,702776	-12 %	-4 %	3 %	12 %	7,72 %	151
64	Warnings	0,089	0,087	-6950,5	66,35	0,04898	0,05653	-117,113037	-11 %	-3 %	1 %	13 %	7,12 %	140
65	OK	0,089	0,089	-7022,2	65,865	0,04934	0,05694	-119,29463	-9 %	-2 %	0 %	9 %	5,10 %	85
66	OK	0,089	0,091	-7072,2	65,451	0,04965	0,0573	-120,992917	-8 %	-1 %	1 %	8 %	4,67 %	70
67	OK	0,089	0,093	-7124,4	65,03	0,04996	0,05766	-122,768061	-6 %	0 %	3 %	7 %	4,14 %	46
68	OK	0,089	0,095	-7171,6	64,636	0,05026	0,05801	-124,424526	-5 %	1 %	4 %	6 %	4,17 %	48
69	OK	0,089	0,097	-7223,3	64,222	0,05058	0,05837	-126,225215	-4 %	1 %	6 %	5 %	4,02 %	41
70	Warnings	0,089	0,099	-7268,9	63,842	0,05087	0,05871	-127,868151	-3 %	2 %	8 %	5 %	4,26 %	52
71	Warnings	0,089	0,101	-7304	63,491	0,05115	0,05903	-129,284455	-2 %	3 %	9 %	6 %	4,97 %	82
72	Warnings	0,089	0,103	-7364	63,075	0,05148	0,05941	-131,311284	0 %	4 %	11 %	2 %	4,26 %	53
73	Warnings	0,089	0,105	-7420,3	62,653	0,05181	0,0598	-133,313401	2 %	5 %	12 %	1 %	4,79 %	72
74	OK	0,089	0,107	-7456,7	62,322	0,05208	0,06011	-134,767761	3 %	6 %	14 %	0 %	5,62 %	107
75	Warnings	0,089	0,109	-7489,6	61,991	0,05236	0,06043	-136,176358	4 %	7 %	15 %	2 %	6,86 %	136
76	Warnings	0,091	0,081	-6888,7	67,044	0,04846	0,05592	-114,722537	-13 %	-5 %	6 %	10 %	8,18 %	160
77	OK	0,091	0,083	-6933,5	66,648	0,04876	0,05627	-116,241959	-11 %	-4 %	4 %	11 %	7,45 %	147
78	Warnings	0,091	0,085	-6971,5	66,26	0,04905	0,0566	-117,644158	-10 %	-3 %	2 %	12 %	6,90 %	137
79	Warnings	0,091	0,087	-7036,5	65,808	0,04938	0,05699	-119,652233	-9 %	-2 %	1 %	9 %	5,21 %	87
80	Warnings	0,091	0,089	-7083,9	65,394	0,04969	0,05734	-121,310881	-8 %	-1 %	1 %	9 %	4,63 %	65
81	Warnings	0,091	0,091	-7118,7	65,018	0,04997	0,05767	-122,694113	-7 %	0 %	3 %	10 %	4,90 %	79
82	OK	0,091	0,093	-7188,8	64,556	0,05032	0,05807	-124,895205	-5 %	1 %	4 %	6 %	3,80 %	30
83	OK	0,091	0,095	-7236,6	64,162	0,05062	0,05842	-126,590134	-4 %	2 %	5 %	5 %	3,90 %	35
84	OK	0,091	0,097	-7286,2	63,762	0,05093	0,05878	-128,354055	-2 %	2 %	7 %	4 %	3,82 %	31

Row	Status	CO2 hydr. rate	rWGS rate	Q kW	FEED kg/sec	N2 mass frac	O2 mass frac.	Q/ [feed-(N2,O2)] kJ/kg	Q/ feed Err.	METH yield Err.	CO2 conv. Err.	H2 conv. Err.	Total Err.	Rank
85	OK	0,091	0,099	-7330,6	63,39	0,05123	0,05912	-129,987995	-1 %	3 %	8 %	3 %	4,07 %	43
86	OK	0,091	0,101	-7371,3	63,022	0,05152	0,05946	-131,567075	0 %	4 %	10 %	3 %	4,53 %	62
87	Warnings	0,091	0,103	-7413,1	62,672	0,0518	0,05979	-133,142298	1 %	5 %	12 %	4 %	5,46 %	99
88	Warnings	0,091	0,105	-7454	62,319	0,05209	0,06012	-134,729074	3 %	6 %	13 %	3 %	6,38 %	125
89	Warnings	0,091	0,107	-7505,6	61,936	0,05241	0,06048	-136,604085	4 %	7 %	15 %	1 %	6,77 %	134
90	OK	0,091	0,109	-7560,5	61,532	0,05274	0,06087	-138,618686	6 %	8 %	16 %	2 %	7,91 %	156
91	Warnings	0,093	0,081	-6955,2	66,543	0,04883	0,05636	-116,807703	-11 %	-4 %	5 %	9 %	7,13 %	142
92	OK	0,093	0,083	-7000,2	66,15	0,04912	0,05669	-118,346165	-10 %	-3 %	3 %	10 %	6,36 %	124
93	Warnings	0,093	0,085	-7050,4	65,736	0,04943	0,05705	-120,036178	-9 %	-2 %	1 %	9 %	5,24 %	90
94	Warnings	0,093	0,087	-7098,6	65,323	0,04974	0,0574	-121,707831	-7 %	-1 %	0 %	9 %	4,38 %	58
95	Warnings	0,093	0,089	-7133,8	64,949	0,05002	0,05773	-123,101208	-6 %	0 %	2 %	10 %	4,65 %	67
96	OK	0,093	0,091	-7203,5	64,486	0,05037	0,05813	-125,300736	-5 %	1 %	3 %	6 %	3,61 %	23
97	OK	0,093	0,093	-7251	64,094	0,05067	0,05848	-126,992455	-3 %	2 %	5 %	5 %	3,72 %	28
98	OK	0,093	0,095	-7300,4	63,696	0,05099	0,05884	-128,753964	-2 %	3 %	6 %	4 %	3,64 %	26
99	OK	0,093	0,097	-7344,6	63,325	0,05128	0,05918	-130,384954	-1 %	4 %	8 %	3 %	3,88 %	33
100	OK	0,093	0,099	-7393,8	62,933	0,05159	0,05954	-132,177778	1 %	4 %	9 %	2 %	4,06 %	42
101	Warnings	0,093	0,101	-7439	62,59	0,05187	0,05986	-133,801849	2 %	5 %	11 %	2 %	5,04 %	83
102	Warnings	0,093	0,103	-7473,9	62,241	0,05215	0,06019	-135,277849	3 %	6 %	13 %	2 %	6,10 %	120
103	Warnings	0,093	0,105	-7514,9	61,893	0,05244	0,06053	-136,880948	4 %	7 %	14 %	2 %	6,98 %	138
104	Warnings	0,093	0,107	-7555,9	61,554	0,05273	0,06085	-138,480769	5 %	8 %	16 %	2 %	7,89 %	154
105	Warnings	0,093	0,109	-7597,7	61,204	0,05302	0,06119	-140,144539	7 %	9 %	17 %	1 %	8,60 %	165
106	Warnings	0,095	0,081	-7023,1	66,04	0,04919	0,05677	-118,951915	-9 %	-3 %	4 %	8 %	5,98 %	116
107	OK	0,095	0,083	-7068,2	65,643	0,04949	0,05712	-120,52603	-8 %	-2 %	2 %	9 %	5,09 %	84
108	OK	0,095	0,085	-7119	65,227	0,04981	0,05748	-122,259004	-7 %	-1 %	0 %	8 %	3,89 %	34
109	OK	0,095	0,087	-7166,6	64,83	0,05011	0,05783	-123,92058	-6 %	0 %	1 %	7 %	3,57 %	22
110	OK	0,095	0,089	-7218,1	64,416	0,05043	0,0582	-125,710567	-4 %	1 %	3 %	6 %	3,43 %	17
111	OK	0,095	0,091	-7263,6	64,033	0,05072	0,05854	-127,347801	-3 %	2 %	4 %	5 %	3,68 %	27
112	Warnings	0,095	0,093	-7297,7	63,679	0,051	0,05886	-128,744563	-2 %	3 %	6 %	7 %	4,38 %	57

Row	Status	CO2 hydr. rate	rWGS rate	Q kW	FEED kg/sec	N2 mass frac	O2 mass frac.	Q/ [feed-(N2,O2)] kJ/kg	Q/ feed Err.	METH yield Err.	CO2 conv. Err.	H2 conv. Err.	Total Err.	Rank
113	OK	0,095	0,095	-7362,2	63,246	0,05134	0,05925	-130,879023	0 %	4 %	7 %	3 %	3,55 %	21
114	OK	0,095	0,097	-7404,9	62,882	0,05163	0,05959	-132,495611	1 %	5 %	9 %	2 %	4,21 %	50
115	OK	0,095	0,099	-7453,7	62,495	0,05195	0,05995	-134,29647	2 %	6 %	10 %	1 %	4,70 %	71
116	OK	0,095	0,101	-7494,6	62,145	0,05223	0,06028	-135,887575	4 %	6 %	12 %	1 %	5,59 %	105
117	Warnings	0,095	0,103	-7538,4	61,79	0,05253	0,06062	-137,567585	5 %	7 %	14 %	0 %	6,45 %	128
118	OK	0,095	0,105	-7586,8	61,411	0,05284	0,06099	-139,409604	6 %	8 %	15 %	2 %	7,91 %	157
119	OK	0,095	0,107	-7623,6	61,076	0,05313	0,06132	-140,951322	7 %	9 %	16 %	2 %	8,81 %	168
120	OK	0,095	0,109	-7654,8	60,762	0,0534	0,06163	-142,355043	8 %	10 %	18 %	1 %	9,50 %	178
121	OK	0,097	0,081	-7087,5	65,551	0,04956	0,05719	-121,043604	-8 %	-1 %	2 %	8 %	4,90 %	77
122	OK	0,097	0,083	-7132,7	65,16	0,04986	0,05754	-122,635628	-7 %	-1 %	1 %	8 %	3,99 %	40
123	Warnings	0,097	0,085	-7168,8	64,793	0,05014	0,05786	-124,038589	-6 %	0 %	1 %	9 %	4,07 %	44
124	OK	0,097	0,087	-7233,5	64,344	0,05048	0,05826	-126,136985	-4 %	1 %	2 %	6 %	3,22 %	13
125	OK	0,097	0,089	-7275	63,968	0,05077	0,0586	-127,695643	-3 %	2 %	4 %	6 %	3,63 %	25
126	Warnings	0,097	0,091	-7319,4	63,601	0,05106	0,05893	-129,304656	-1 %	3 %	6 %	6 %	3,96 %	37
127	Warnings	0,097	0,093	-7374,4	63,19	0,05138	0,0593	-131,227204	0 %	4 %	7 %	3 %	3,44 %	18
128	Warnings	0,097	0,095	-7428,7	62,774	0,05171	0,05968	-133,176567	1 %	5 %	8 %	0 %	3,63 %	24
129	OK	0,097	0,097	-7464,8	62,443	0,05198	0,05999	-134,62003	3 %	6 %	10 %	1 %	4,86 %	76
130	Warnings	0,097	0,099	-7497,8	62,112	0,05226	0,06031	-136,025726	4 %	7 %	12 %	2 %	6,08 %	119
131	OK	0,097	0,101	-7557,3	61,706	0,0526	0,0607	-138,121262	5 %	7 %	13 %	1 %	6,71 %	132
132	OK	0,097	0,103	-7597	61,366	0,05288	0,06103	-139,715341	6 %	8 %	14 %	2 %	7,71 %	150
133	OK	0,097	0,105	-7643,1	61,001	0,05319	0,06139	-141,509327	8 %	9 %	16 %	3 %	9,08 %	171
134	OK	0,097	0,107	-7674,9	60,669	0,05348	0,06172	-142,973968	9 %	10 %	17 %	3 %	9,97 %	181
135	Warnings	0,097	0,109	-7712,3	60,361	0,05375	0,06203	-144,498417	10 %	11 %	19 %	3 %	10,70 %	189
136	Warnings	0,099	0,081	-7160,1	65,029	0,04993	0,05762	-123,376155	-6 %	0 %	2 %	5 %	3,35 %	15
137	OK	0,099	0,083	-7201,7	64,662	0,05023	0,05797	-124,886334	-5 %	1 %	0 %	6 %	2,94 %	10
138	OK	0,099	0,085	-7234,5	64,304	0,05051	0,05829	-126,238566	-4 %	1 %	2 %	8 %	3,72 %	29
139	Warnings	0,099	0,087	-7276,2	63,942	0,05079	0,05862	-127,77258	-3 %	2 %	4 %	8 %	4,27 %	54
140	OK	0,099	0,089	-7344,4	63,491	0,05115	0,05903	-129,99893	-1 %	3 %	5 %	4 %	3,17 %	11

Row	Status	CO2 hydr. rate	rWGS rate	Q kW	FEED kg/sec	N2 mass frac	O2 mass frac.	Q/ [feed-(N2,O2)] kJ/kg	Q/ feed Err.	METH yield Err.	CO2 conv. Err.	H2 conv. Err.	Total Err.	Rank
141	Warnings	0,099	0,091	-7387,6	63,122	0,05144	0,05937	-131,620365	0 %	4 %	6 %	3 %	3,49 %	19
142	OK	0,099	0,093	-7436,5	62,732	0,05175	0,05973	-133,418867	2 %	5 %	8 %	1 %	3,97 %	38
143	OK	0,099	0,095	-7473	62,378	0,05204	0,06006	-134,927173	3 %	6 %	9 %	2 %	4,90 %	78
144	Warnings	0,099	0,097	-7510,5	62,047	0,05231	0,06038	-136,417272	4 %	7 %	11 %	3 %	6,07 %	118
145	OK	0,099	0,099	-7570,5	61,639	0,05265	0,06076	-138,530779	6 %	8 %	12 %	2 %	6,75 %	133
146	OK	0,099	0,101	-7613,1	61,29	0,05294	0,0611	-140,203714	7 %	9 %	14 %	2 %	7,87 %	153
147	OK	0,099	0,103	-7657,2	60,936	0,05325	0,06145	-141,94062	8 %	9 %	15 %	4 %	9,13 %	174
148	OK	0,099	0,105	-7695,7	60,61	0,05353	0,06178	-143,519763	9 %	10 %	17 %	4 %	10,06 %	183
149	OK	0,099	0,107	-7731,6	60,284	0,05381	0,06211	-145,06985	11 %	11 %	19 %	4 %	10,96 %	191
150	Warnings	0,099	0,109	-7771,1	59,967	0,05409	0,06242	-146,678225	12 %	12 %	20 %	4 %	11,96 %	201
151	Warnings	0,101	0,081	-7225,4	64,545	0,0503	0,05804	-125,544641	-4 %	1 %	1 %	4 %	2,50 %	4
152	OK	0,101	0,083	-7266,1	64,186	0,05059	0,05839	-127,049936	-3 %	2 %	1 %	5 %	2,77 %	7
153	OK	0,101	0,085	-7298,5	63,836	0,05087	0,05871	-128,402603	-2 %	2 %	3 %	7 %	3,54 %	20
154	Warnings	0,101	0,087	-7339,1	63,481	0,05115	0,05904	-129,92823	-1 %	3 %	5 %	7 %	4,08 %	45
155	OK	0,101	0,089	-7405,8	63,038	0,05151	0,05945	-132,143966	1 %	4 %	6 %	3 %	3,34 %	14
156	Warnings	0,101	0,091	-7448	62,677	0,0518	0,05978	-133,756519	2 %	5 %	7 %	2 %	4,15 %	47
157	OK	0,101	0,093	-7496,2	62,293	0,05211	0,06014	-135,553036	3 %	6 %	9 %	0 %	4,62 %	64
158	OK	0,101	0,095	-7532,3	61,946	0,0524	0,06047	-137,06384	4 %	7 %	10 %	0 %	5,54 %	103
159	Warnings	0,101	0,097	-7568,8	61,622	0,05267	0,06079	-138,54461	6 %	8 %	12 %	1 %	6,71 %	131
160	OK	0,101	0,099	-7628	61,22	0,053	0,06117	-140,658212	7 %	9 %	13 %	3 %	7,94 %	159
161	OK	0,101	0,101	-7667,1	60,889	0,05328	0,0615	-142,245952	8 %	10 %	15 %	3 %	8,90 %	170
162	OK	0,101	0,103	-7711,9	60,534	0,05359	0,06185	-144,026089	10 %	10 %	16 %	5 %	10,25 %	184
163	Warnings	0,101	0,105	-7750,8	60,21	0,05387	0,06217	-145,628462	11 %	11 %	18 %	5 %	11,23 %	195
164	Warnings	0,101	0,107	-7786,3	59,898	0,05415	0,06249	-147,156701	12 %	12 %	19 %	5 %	12,10 %	203
165	Warnings	0,101	0,109	-7824,4	59,606	0,05441	0,06279	-148,697095	13 %	13 %	21 %	4 %	12,90 %	211
166	Warnings	0,103	0,081	-7288,1	64,054	0,05066	0,05847	-127,718247	-3 %	2 %	0 %	3 %	2,01 %	1
167	OK	0,103	0,083	-7329,5	63,717	0,05096	0,05881	-129,215114	-2 %	3 %	2 %	4 %	2,60 %	6
168	OK	0,103	0,085	-7361,6	63,374	0,05123	0,05913	-130,571611	-1 %	4 %	4 %	5 %	3,37 %	16

Row	Status	CO2 hydr. rate	rWGS rate	Q kW	FEED kg/sec	N2 mass frac	O2 mass frac.	Q/ [feed-(N2,O2)] kJ/kg	Q/ feed Err.	METH yield Err.	CO2 conv. Err.	H2 conv. Err.	Total Err.	Rank
169	Warnings	0,103	0,087	-7401	63,026	0,05151	0,05945	-132,084685	1 %	4 %	6 %	6 %	4,21 %	49
170	OK	0,103	0,089	-7466,4	62,592	0,05187	0,05986	-134,28996	2 %	5 %	7 %	2 %	3,99 %	39
171	Warnings	0,103	0,091	-7507,6	62,239	0,05216	0,06019	-135,893586	4 %	6 %	8 %	1 %	4,80 %	73
172	OK	0,103	0,093	-7555	61,862	0,05247	0,06055	-137,688152	5 %	7 %	10 %	1 %	5,61 %	106
173	OK	0,103	0,095	-7590,5	61,521	0,05275	0,06088	-139,199386	6 %	8 %	11 %	1 %	6,50 %	129
174	Warnings	0,103	0,097	-7626,2	61,202	0,05302	0,06119	-140,673258	7 %	9 %	13 %	0 %	7,34 %	145
175	OK	0,103	0,099	-7683,8	60,81	0,05335	0,06157	-142,764927	9 %	10 %	14 %	4 %	9,12 %	173
176	OK	0,103	0,101	-7726,9	60,462	0,05365	0,06192	-144,495774	10 %	11 %	16 %	5 %	10,35 %	188
177	OK	0,103	0,103	-7761	60,144	0,05393	0,06224	-146,001607	11 %	11 %	17 %	5 %	11,23 %	193
178	Warnings	0,103	0,105	-7793	59,845	0,0542	0,06255	-147,43297	12 %	12 %	19 %	4 %	11,91 %	200
179	Warnings	0,103	0,107	-7827,5	59,541	0,05447	0,06287	-148,939582	13 %	13 %	21 %	4 %	12,74 %	209
180	OK	0,103	0,109	-7887,5	59,157	0,05481	0,06326	-151,181738	15 %	14 %	22 %	8 %	14,86 %	219
181	Warnings	0,105	0,081	-7348,6	63,615	0,05103	0,0589	-129,784527	-1 %	3 %	2 %	3 %	2,11 %	2
182	OK	0,105	0,083	-7389,9	63,265	0,05132	0,05923	-131,325966	0 %	4 %	3 %	3 %	2,58 %	5
183	OK	0,105	0,085	-7421,2	62,926	0,05159	0,05954	-132,681587	1 %	5 %	5 %	5 %	3,83 %	32
184	Warnings	0,105	0,087	-7460,9	62,583	0,05187	0,05987	-134,214406	2 %	5 %	7 %	5 %	4,91 %	80
185	OK	0,105	0,089	-7526	62,152	0,05222	0,06027	-136,436852	4 %	6 %	8 %	0 %	4,65 %	66
186	Warnings	0,105	0,091	-7566,3	61,807	0,05251	0,0606	-138,032006	5 %	7 %	9 %	0 %	5,46 %	100
187	OK	0,105	0,093	-7612,9	61,436	0,05282	0,06096	-139,824807	7 %	8 %	11 %	2 %	6,80 %	135
188	OK	0,105	0,095	-7648,5	61,102	0,0531	0,06129	-141,344342	8 %	9 %	12 %	2 %	7,70 %	149
189	Warnings	0,105	0,097	-7682,7	60,789	0,05337	0,0616	-142,799924	9 %	10 %	14 %	1 %	8,40 %	163
190	OK	0,105	0,099	-7740	60,404	0,0537	0,06198	-144,898847	10 %	11 %	15 %	5 %	10,26 %	185
191	OK	0,105	0,101	-7776,9	60,086	0,05398	0,0623	-146,460589	12 %	12 %	17 %	5 %	11,23 %	194
192	OK	0,105	0,103	-7820,7	59,74	0,05429	0,06266	-148,247566	13 %	13 %	18 %	7 %	12,61 %	207
193	OK	0,105	0,105	-7853,5	59,428	0,05457	0,06298	-149,753022	14 %	13 %	20 %	7 %	13,52 %	213
194	Warnings	0,105	0,107	-7885,9	59,137	0,05483	0,06328	-151,208728	15 %	14 %	21 %	6 %	14,23 %	216
195	OK	0,105	0,109	-7939,5	58,779	0,05515	0,06365	-153,283399	17 %	15 %	23 %	10 %	16,05 %	223
196	Warnings	0,107	0,081	-7410,8	63,154	0,0514	0,05932	-131,954348	1 %	4 %	3 %	2 %	2,21 %	3

Row	Status	CO2 hydr. rate	rWGS rate	Q kW	FEED kg/sec	N2 mass frac	O2 mass frac.	Q/ [feed-(N2,O2)] kJ/kg	Q/ feed Err.	METH yield Err.	CO2 conv. Err.	H2 conv. Err.	Total Err.	Rank
197	OK	0,107	0,083	-7452,9	62,811	0,05168	0,05964	-133,520133	2 %	5 %	4 %	2 %	3,21 %	12
198	Warnings	0,107	0,085	-7489	62,471	0,05196	0,05997	-134,989627	3 %	6 %	6 %	3 %	4,32 %	56
199	Warnings	0,107	0,087	-7527,9	62,132	0,05224	0,06029	-136,521079	4 %	7 %	8 %	3 %	5,35 %	96
200	Warnings	0,107	0,089	-7568,4	61,787	0,05253	0,06062	-138,120848	5 %	7 %	9 %	3 %	6,20 %	121
201	Warnings	0,107	0,091	-7608,8	61,454	0,05281	0,06095	-139,705074	6 %	8 %	11 %	3 %	7,12 %	141
202	Warnings	0,107	0,093	-7650,2	61,102	0,05311	0,06129	-141,376081	8 %	9 %	12 %	2 %	7,78 %	152
203	Warnings	0,107	0,095	-7691,3	60,777	0,05339	0,06161	-142,994224	9 %	10 %	14 %	2 %	8,63 %	166
204	Warnings	0,107	0,097	-7732,5	60,427	0,05369	0,06196	-144,699694	10 %	11 %	15 %	0 %	9,18 %	175
205	OK	0,107	0,099	-7792,5	60,011	0,05405	0,06238	-146,961279	12 %	12 %	16 %	5 %	11,38 %	196
206	OK	0,107	0,101	-7831,4	59,69	0,05434	0,06271	-148,594733	13 %	13 %	18 %	6 %	12,44 %	206
207	OK	0,107	0,103	-7874,3	59,351	0,05464	0,06306	-150,37251	15 %	14 %	19 %	8 %	13,81 %	215
208	OK	0,107	0,105	-7910	59,045	0,05491	0,06337	-151,936645	16 %	14 %	21 %	8 %	14,76 %	218
209	Warnings	0,107	0,107	-7947,6	58,739	0,05519	0,0637	-153,563014	17 %	15 %	22 %	9 %	15,81 %	221
210	OK	0,107	0,109	-7990,2	58,407	0,0555	0,06405	-155,378279	18 %	16 %	24 %	11 %	17,27 %	225
211	Warnings	0,109	0,081	-7472,7	62,704	0,05176	0,05973	-134,128861	2 %	5 %	4 %	1 %	2,86 %	9
212	OK	0,109	0,083	-7510,6	62,367	0,05204	0,06006	-135,627664	3 %	6 %	5 %	1 %	3,94 %	36
213	Warnings	0,109	0,085	-7551	62,024	0,05233	0,06039	-137,210336	5 %	7 %	7 %	1 %	4,86 %	75
214	OK	0,109	0,087	-7598,8	61,646	0,05264	0,06076	-139,030705	6 %	8 %	8 %	1 %	5,68 %	110
215	OK	0,109	0,089	-7636,1	61,31	0,05293	0,06108	-140,577112	7 %	9 %	10 %	1 %	6,58 %	130
216	OK	0,109	0,091	-7664	60,992	0,0532	0,0614	-141,917926	8 %	9 %	12 %	0 %	7,27 %	143
217	Warnings	0,109	0,093	-7705,4	60,672	0,05348	0,06172	-143,534027	9 %	10 %	13 %	0 %	8,28 %	162
218	OK	0,109	0,095	-7766	60,27	0,05382	0,06212	-145,752873	11 %	11 %	14 %	5 %	10,28 %	186
219	OK	0,109	0,097	-7811,8	59,922	0,05412	0,06247	-147,572599	12 %	12 %	16 %	7 %	11,71 %	197
220	OK	0,109	0,099	-7842,1	59,626	0,05439	0,06277	-148,977036	13 %	13 %	17 %	6 %	12,36 %	205
221	Warnings	0,109	0,101	-7878,9	59,323	0,05466	0,06308	-150,536992	15 %	14 %	19 %	6 %	13,28 %	212
222	OK	0,109	0,103	-7927,1	58,97	0,05498	0,06345	-152,485043	16 %	15 %	20 %	9 %	14,95 %	220
223	OK	0,109	0,105	-7961,3	58,673	0,05525	0,06377	-154,019772	17 %	16 %	22 %	9 %	15,87 %	222
224	OK	0,109	0,107	-8002,6	58,349	0,05555	0,06412	-155,794315	19 %	16 %	23 %	11 %	17,24 %	224

Row	Status	CO2 hydr. rate	rWGS rate	Q kW	FEED kg/sec	N2 mass frac	O2 mass frac.	Q/ [feed-(N2,O2)] kJ/kg	Q/ feed Err.	METH yield Err.	CO2 conv. Err.	H2 conv. Err.	Total Err.	Rank
225	Warnings	0,109	0,109	-8039,4	58,054	0,05583	0,06444	-157,411295	20 %	17 %	25 %	11 %	18,17 %	226
226	OK	0,099	0,087	-7301,1	63,858	0,05084	0,05868	-128,396323	-2 %	2 %	3 %	4 %	2,82 %	8

Appendix 2. Stream data for the CO_2 capture process extracted from the Aspen Plus model.

Stream		AIR-IN	AIR-OUT	CH4-IN	CO2	COLDWAT	H2O-IN	LIME-IN	LIME-OUT	MOISTCO2
Phase:		Vapor	Vapor	Vapor	Mixed	Liquid	Liquid	All	All	Vapor
Mass frac.										
CO2		0,000613	0,000156	0	0,96423	0	0	0	0	0,8857832
O2		0,222857	0,222103	0	0,018882	0	0	0	0	0,0173414
N2		0,770257	0,767654	0	0,014887	0	0	0	0	0,0136724
H2O		0,006273	0,010087	0	0,002001	1	1	0,706	0,707469	0,0832028
CACO3		0	0	0	0	0	0	0	0	0
CAO		0	0	0	0	0	0	0	0	0
CA(OH)2		0	0	0	0	0	0	0,282	0,288083	0
K2CO3		0	0	0	0	0	0	0,0075	0,003473	0
CH4		0	0	1	0	0	0	0	0	0
KOH		0	0	0	0	0	0	0,0045	0,000975	0
Mole Flow	KMOL/HR	2251250	2264390	189,1546	919,726	44406,75	7592,766	8587,019	8436,261	1115,416
Mass Flow	TONNE/HR	64649,11	64868,28	3,034563	39,7427	800	136,7858	199,0986	195,2786	43,2744
Volume Flow	CUM/MIN	914405	900177	76,71462	6,191515	17,64558	3,017081	3,517228	3,585226	508,8301
Temperature	C	20	13,81139	20	40	20	20	20	66,9112	57,4771
Pressure	BAR	1	1	1	50	1	1	1	1	1
Vapor frac.		1	1	1	0,997832	0	0	0	0	1
Liquid frac.		0	0	0	0,002168	1	1	0,908635	0,909015	0
Solid frac.		0	0	0	0	0	0	0,091365	0,090985	0
Enthalpy	KJ/KG	-95,0335	-148,499	-4657,28	-8687,82	-15893,12	-15893,1	-15071,9	-14958,8	-9007,134
Entropy	J/KG-K	131,7672	106,8574	-5057,49	-726,962	-9152,977	-9152,98	-7615,33	-7137,38	92,70153
Density	KG/CUM	1,178345	1,201028	0,659275	106,9816	755,6188	755,6188	943,4449	907,7928	1,417447

Stream		O2-IN	S1	S10	S11	S12	S13	S14	S16	S17	S18
Phase:		Vapor	All	Solid	All	All	All	Solid	Liquid	Liquid	Solid
Mass frac.											
CO2		0	0	0	0	0	0	0	0,002278	0,006069	0
O2		0,956	0	0	0	0	0	0	2,08E-06	5,74E-06	0
N2		0,044	0	0	0	0	0	0	7,25E-07	2,01E-06	0
H2O		0	0,958915	0	0,887	0,229933	0,887	0	0,997719	0,993924	0
CACO3		0	0	0,034721	0	0	0	0	0	0	0,034721
CAO		0	0	0,953222	0	0,089841	0	0,116666	0	0	0,953222
CA(OH)2		0	0,038456	0	0	0,67265	0	0,873495	0	0	0
K2CO3		0	0,001325	0,012058	0,057	0,007576	0,057	0,009839	0	0	0,012058
CH4		0	0	0	0	0	0	0	0	0	0
KOH		0	0,001304	0	0,056	0	0,056	0	0	0	0
Mole Flow	KMOL/HR	422,8858	7851,784	700,949	5074440	1503,768	1613090	687,0001	173,0888	16,56237	700,949
Mass Flow	TONNE/HR	13,44766	145,999	40,20939	100193	63,99391	31850	49,2796	3,122448	0,29945	40,20939
Volume Flow	CUM/MIN	171,7161	3,209029	0,205748	2044,666	642,9347	649,9703	0,363094	0,069796	0,006684	0,205705
Temperature	C	20	53,63497	898,7882	20	295,8519	20	85	40	40	674
Pressure	BAR	1	1	1	1	1	1	1	2,659148	7,071068	1
Vapor frac.		1	0	0	0	0,543148	0	0	0	0	0
Liquid frac.		0	0,989739	0	0,972149	0	0,972149	0	1	1	0
Solid frac.		0	0,010261	1	0,027851	0,456852	0,027851	1	0	0	1
Enthalpy	KJ/KG	-4,87645	-15634,7	-10498	-14996,4	-12730,9	-14996,4	-12956,4	-15793,1	-15767,9	-10717,2
Entropy	J/KG-K	38,90964	-8489,68	-656,29	-8394,8	-2500,72	-8394,8	-3488,64	-8854,74	-8826,86	-863,789
Density	KG/CUM	1,305222	758,2718	3257,176	816,704	1,658901	816,704	2262,025	745,6125	746,6916	3257,856

Stream		S19	S2	S20	S21	S22	S23	S24	S25	S3	S32
Phase:		Vapor	Mixed	Liquid	All	Liquid	All	Solid	Solid	All	All
Mass frac.											
CO2		0	0,000149	0,015534	0,000339	0,000523	0	0	0	1,57E-07	0
O2		0,956	0,212502	1,62E-05	3,66E-07	5,66E-07	0	0	0	7,50E-06	0
N2		0,044	0,73447	5,73E-06	1,38E-07	2,13E-07	0	0	0	1,02E-05	0
H2O		0	0,047371	0,984444	0,647067	0,999476	0,887	0	0	0,872582	2,19E-06
CACO3		0	0	0	0,32263	0	0	0	0	0	0,9931
CAO		0	0	0	0	0	0	0,987509	0,116666	0	0
CA(OH)2		0	0	0	0,02595	0	0	0	0,873495	0	0
K2CO3		0	0,004016	0	0,003135	0	0,057	0,012492	0,009839	0,092898	0,006898
CH4		0	0	0	0	0	0	0	0	0	0
KOH		0	0,001491	0	0,00088	0	0,056	0	0	0,034502	0
Mole Flow	KMOL/HR	422,8858	2410120	6,038661	8554,41	7772,892	159537	687,0001	687,0001	145731	700,9575
Mass Flow	TONNE/HR	13,44766	67799,11	0,109797	216,3622	140,0741	3150	38,8133	49,2796	2930,83	70,2899
Volume Flow	CUM/MIN	555,1874	900236	0,002442	3,642381	3,175268	64,28278	0,197009	0,479302	58,84473	0,4488
Temperature	C	674	13,81139	40	53,63497	57,4771	20	674	295,8519	13,81139	650
Pressure	BAR	1	1	18,80302	1	1	1	1	1	1	1
Vapor frac.		1	0,939534	0	0	0	0	0	0	0	1,22E-05
Liquid frac.		0	0,058901	1	0,908641	1	0,972149	0	0	0,974114	0
Solid frac.		0	0,001565	0	0,091359	0	0,027851	1	1	0,025886	0,999988
Enthalpy	KJ/KG	654,3139	-787,361	-15705,1	-14456,1	-15730,9	-14996,4	-10693,2	-12679	-14927,3	-11387,7
Entropy	J/KG-K	1201,311	-259,263	-8758,92	-6557,92	-8638,94	-8394,8	-842,23	-2881,65	-8362,64	-1489,9
Density	KG/CUM	0,403697	1,25521	749,4079	990,022	735,2352	816,704	3283,552	1713,589	830,1026	2610,293

Stream		S34	S4	S40	S6	S7	S8	S9	SEED-IN	SEED-OUT
Phase:		Vapor	Solid	Vapor	All	All	All	Vapor	Solid	Solid
Mass frac.										
CO2		0,824802	0	0,998514	1,31E-08	0	0,442596	0,824802	0	0
O2		0,016118	0	0,00108	6,28E-07	0	0,008649	0,016118	0	0
N2		0,012708	0	0,000406	8,55E-07	0	0,006819	0,012708	0	0
H2O		0,146373	0	0	0,884762	2,19E-06	0,078545	0,146373	0	0
CACO3		0	0,91326	0	0,001951	0,9931	0,016089	0	1	1
CAO		0	0	0	0	0	0,441714	0	0	0
CA(OH)2		0	0,075119	0	0,000161	0	0	0	0	0
K2CO3		0	0,009075	0	0,057031	0,006898	0,005587	0	0	0
CH4		0	0	0	0	0	0	0	0	0
KOH		0	0,002546	0	0,056093	0	0	0	0	0
Mole Flow	KMOL/HR	1295,541	766,0783	1,668447	1768090	700,9575	1996,49	1295,541	15,44051	13,94882
Mass Flow	TONNE/HR	46,56273	74,7427	0,073381	34979,93	70,2899	86,77212	46,56273	1,545397	1,396098
Volume Flow	CUM/MIN	1073,336	0,465222	0,752821	712,1828	0,432276	2104,459	2104,253	0,00949	0,0086961
Temperature	C	325	19,08555	53,63497	19,08555	53,63497	898,7882	898,7882	20	674
Pressure	BAR	1	1	1	1	1	1	1	1	1
Vapor frac.		1	0	1	0	0	0,648909	1	0	0
Liquid frac.		0	0	0	0,971628	1,22E-05	0	0	0	0
Solid frac.		0	1	0	0,028372	0,999988	0,351091	0	1	1
Enthalpy	KJ/KG	-9005,5	-12116,4	-8904,23	-14991	-12013,5	-9286,08	-8239,48	-12067,3	-11385,1
Entropy	J/KG-K	640,7114	-2744,56	148,3475	-8392,63	-2551,58	516,8835	1529,981	-2645,32	-1463,161
Density	KG/CUM	0,723022	2677,673	1,624584	818,6084	2710,072	0,687209	0,368799	2714,015	2675,723

Stream		SORB-IN	SORB-OUT	STEAM-IN	STEAM-OU
Phase:		All	All	Liquid	Vapor
Mass frac.					
CO2		0	1,32E-08	0	0
O2		0	6,29E-07	0	0
N2		0	8,56E-07	0	0
H2O		0,887	0,8866563	1	1
CACO3		0	0	0	0
CAO		0	0	0	0
CA(OH)2		0	0	0	0
K2CO3		0,057	0,0571341	0	0
CH4		0	0	0	0
KOH		0,056	0,0562081	0	0
Mole Flow	KMOL/HR	1772630	1767330	1397,736	816,7681
Mass Flow	TONNE/HR	35000	34905,19	25,18061	14,71431
Volume Flow	CUM/MIN	714,2531	711,7176	0,557323	642,4554
Temperature	C	20	19,08555	25	295,8519
Pressure	BAR	1	1	1	1
Vapor frac.		0	0	0	1
Liquid frac.		0,972149	0,9720489	1	0
Solid frac.		0,027851	0,0279511	0	0
Enthalpy	KJ/KG	-14996,4	-14997,16	-15871,8	-12904,38
Entropy	J/KG-K	-8394,8	-8404,716	-9080,76	-1224,95
Density	KG/CUM	816,704	817,3932	753,0221	0,3817205

Appendix 3. Stream data for the synthesis and distillation processes extracted from the Aspen Plus model.

Stream		AIR-IN	CO2	COOLING1	COOLING2	DISTIL	DISTIL2	DISTIL3	FLUE	H2
Phase:		Vapor	Mixed	Liquid	Mixed	Liquid	Liquid	Vapor	Vapor	Vapor
Mass frac.										
H2		0	0	0	0	0,0003366	1,54E-06	2,18E-06	0	1
CO2		0	0,965918	0	0	0,0342984	0,002607	0,003698	0,158859	0
CH3OH		0	0	0	0	0,6100105	0,628916	0,892168	0	0
H2O		0	0,001999	1	1	0,3547318	0,368473	0,104128	0,157892	0
CO		0	0	0	0	0,0001636	7,93E-07	1,12E-06	0	0
N2		0,77	0,014895	0	0	0,0002149	1,04E-06	1,47E-06	0,632323	0
O2		0,23	0,017188	0	0	0,0002442	1,17E-06	1,67E-06	0,050925	0
Mole Flow	KMOL/HR	1622,157	918,662	1665,253	1665,253	1391,115	1351,422	800	2115,672	2513,275
Mass Flow	TONNE/HR	46,78238	39,72142	30	30	35,04439	33,66671	23,73268	57,90401	5,066461
Volume Flow	CUM/MIN	670,2504	6,175714	0,6617093	203,5277	0,9002168	0,871617	375,6536	1150,914	37,60234
Temperature	C	25	40	20	99,57755	39,62802	35,79776	71,07249	120	45
Pressure	BAR	1	50	1	1	45	1	1	1	30
Vapor frac.		1	0,997834	0	0,2379777	0	0	1	1	1
Liquid frac.		0	0,002167	1	0,7620223	1	1	0	0	0
Solid frac.		0	0	0	0	0	0	0	0	0
Enthalpy	KJ/KG	-0,21615	-8703,06	-15893,12	-15017,28	-10461,31	-10544,9	-6962,44	-3431,77	300,8213
Entropy	J/KG-K	150,1789	-728,401	-9152,977	-6690,381	-7601,441	-7859,7	-3523,91	245,4871	-13072,96
Density	KG/CUM	1,163306	107,1979	755,6188	2,456668	648,8138	643,7599	1,052951	0,838522	2,245632

Stream		MEOH	PURGE	PURGE2	REAC-IN	REAC-OUT	RECYCLE	RECYCLE2	RECYCLE3	S1
Phase:		Vapor	Vapor	Vapor	Vapor	Vapor	Vapor	Vapor	Vapor	Vapor
Mass frac.										
H2		2,44E-06	0,0989409	0,008524	0,101703	0,083912	0,098941	0,0989409	0,0989409	0,087741
CO2		0,00412978	0,712927	0,808761	0,740924	0,6094937	0,712927	0,712927	0,712927	0,724798
CH3OH		0,9957503	0,0135515	0,148004	0,010912	0,1044607	0,013552	0,0135515	0,0135515	0,030207
H2O		0,00011269	0,001863	0,018945	0,001846	0,0556461	0,001863	0,001863	0,00186303	0,003979
CO		1,26E-06	0,0435824	0,004141	0,035093	0,0369647	0,043582	0,0435824	0,0435824	0,038697
N2		1,64E-06	0,059948	0,005441	0,050844	0,0508438	0,059948	0,059948	0,059948	0,053196
O2		1,86E-06	0,0691868	0,006183	0,058679	0,0586789	0,069187	0,0691868	0,0691868	0,061382
Mole Flow	KMOL/HR	662,5265	698,2952	39,69243	16699,55	15357	13965,9	13267,61	13267,61	737,9876
Mass Flow	TONNE/HR	21,25	9,74395	1,377676	229,9229	229,9229	194,879	185,135	185,135	11,12163
Volume Flow	CUM/MIN	304,2505	6,723952	16,90673	230,4895	222,1597	134,479	127,7551	119,2449	318,7557
Temperature	C	64,15121	39,62802	35,79776	225	250	39,62802	39,62802	51,11508	38,62004
Pressure	BAR	1	45	1	50	50	45	45	50	1
Vapor frac.		1	1	1	1	1	1	1	1	1
Liquid frac.		0	0	0	0	0	0	0	0	0
Solid frac.		0	0	0	0	0	0	0	0	0
Enthalpy	KJ/KG	-6232,073	-6625,9	-8419,92	-6397,67	-6512,015	-6625,9	-6625,9	-6598,271	-6848,13
Entropy	J/KG-K	-3850,605	-1479,181	-282,304	-531,151	-691,2754	-1479,181	-1479,181	-1455,204	682,9295
Density	KG/CUM	1,164063	24,15234	1,358114	16,6257	17,24908	24,15234	24,15234	25,87603	0,581513

Stream		S11	S12	S13	S14	S3	S4	S7	S8	SGIN
Phase:		Vapor	Liquid	Mixed	Liquid	Vapor	Vapor	Liquid	Liquid	Vapor
Mass frac.										
H2		1	6,83E-55	0,083912	2,64E-54	0,101703	0	0	0	0
CO2		0	6,83E-41	0,609492	1,02E-38	0,740924	0,158859	0	0	0
CH3OH		0	7,21E-07	0,104462	0,00042605	0,010912	0	0	0	0
H2O		0	0,999999	0,055646	0,9995739	0,001846	0,157892	1	1	1
CO		0	3,30E-56	0,036965	8,07E-55	0,035093	0	0	0	0
N2		0	4,87E-57	0,050844	2,43E-55	0,050844	0,632323	0	0	0
O2		0	4,55E-56	0,058679	1,31E-54	0,058679	0,050925	0	0	0
Mole Flow	KMOL/HR	2513,275	551,4222	15357,02	1802,727	16699,55	2115,672	1665,253	1665,253	1665,253
Mass Flow	TONNE/HR	5,066461	9,934028	229,9234	32,48268	229,9229	57,90401	30	30	30
Volume Flow	CUM/MIN	22,48031	0,233597	122,064	0,7638781	147,2739	5661,61	0,663998	0,663991	204,022
Temperature	C	40	99,5775	40	99,53335	45,2041	1658,345	25,10732	25	180
Pressure	BAR	50	1	50	1	50	1	5	1	5
Vapor frac.		1	0	0,908847	0	1	1	0	0	1
Liquid frac.		0	1	0,091153	1	0	0	1	1	0
Solid frac.		0	0	0	0	0	0	0	0	0
Enthalpy	KJ/KG	238,8208	-15557,7	-7210,49	-15554,31	-6811,237	-1315,5	-15870,9	-15871,8	-13144,3
Entropy	J/KG-K	-15426,4	-8140,2	-2465,88	-8139,24	-1561,864	2353,414	-9079,6	-9080,76	-2432,87
Density	KG/CUM	3,756221	708,7738	31,39383	708,7231	26,01988	0,170458	753,0143	753,0221	2,450716

Stream		WASTEWAT
Phase:		Mixed
Mass frac.		
H2		2,18E-54
CO2		7,82E-39
CH3OH		0,00032644
H2O		0,9996736
CO		6,26E-55
N2		1,87E-55
O2		1,01E-54
Mole Flow	KMOL/HR	2354,149
Mass Flow	TONNE/HR	42,41671
Volume Flow	CUM/MIN	0,9974956
Temperature	C	99,54368
Pressure	BAR	1
Vapor frac.		1,74E-08
Liquid frac.		1
Solid frac.		0
Enthalpy	KJ/KG	-15555,1
Entropy	J/KG-K	-8139,445
Density	KG/CUM	708,7201